RC22944 (W0310-160) October 28, 2003
Mathematics

IBM Research Report

Computing Invariant Manifolds by Integrating Fat Trajectories

Michael E. Henderson
IBM Research Division
Thomas J. Watson Research Center
P.O. Box 218
Yorktown Heights, NY 10598

Research Division
Almaden - Austin - Beijing - Haifa - India - T. J. Watson - Tokyo - Zurich

COMPUTING INVARIANT MANIFOLDS BY INTEGRATING FAT TRAJECTORIES

MICHAEL E. HENDERSON†

Abstract. We present a new method of computing a well distributed set of points on k-dimensional manifolds which are invariant under a flow. The method uses on chains of local approximations along trajectories (fat trajectories) to cover the manifold with well spaced points. Points between two diverging fat trajectories are interpolated by either interpolating over a certain dual simplex, or by solving a two point boundary value problem.

We derive formulae for the evolution of a second local approximation of the invariant manifold along a trajectory, show that interpolation points in the cleft where k (the dimension of the manifold) trajectories diverge will exist, and apply the method to the stable manifold of the origin in the "standard" Lorenz system.

Key words. Invariant Manifolds, Numerical Analysis, Lorenz manifold

AMS subject classifications. 37C10, 34K19, 37M20

1. Introduction.

Given a flow

$$\frac{\mathrm{d}u^i}{\mathrm{d}t} = F^i(\mathbf{u}), \qquad \mathbf{u} \in \mathbb{R}^n, \qquad \mathbf{F} : \mathbb{R}^n \to \mathbb{R}^n,$$

the k-dimensional invariant manifold $M_{\mathbf{c}}$ generated by a smooth $(k-1)$-dimensional manifold of starting points $\mathbf{c}(\sigma) \in \mathbb{R}^n$, $\mathbf{F}$ nowhere tangent to $\mathbf{c}$, consists of the union of the forward and backward images of the starting points under the flow:

$$\begin{aligned} u^i_+(t,\sigma) &= c^i(\sigma) + \int_0^t F^i(\mathbf{u}(\tau,\sigma))\mathrm{d}\tau \\ u^i_-(t,\sigma) &= c^i(\sigma) - \int_0^t F^i(\mathbf{u}(\tau,\sigma))\mathrm{d}\tau \\ M_{\mathbf{c}} &= \mathbf{u}_- \bigcup \mathbf{u}_+ \end{aligned} \tag{1.1}$$

This paper describes an algorithm for finding a well distributed set of points on such a manifold.

This definition is sometimes written using the "flow" $\mathbf{u}(t,\sigma) = \phi^t(\mathbf{c}(\sigma))$, but we wish to emphasize that it is a surface and that on that surface t is a parameter just like σ. What is special about time is that the tangent of the surface in the t direction is known explicitly at any point, while the other tangents are not. $M_{\mathbf{c}}$ may be infinite in extent, and may have infinite area inside a finite region, so we restrict the invariant manifold to a computational domain, for example, $t \in [-T, T]$, $\sigma \in \Omega_\sigma$, and $M_{\mathbf{c}} \cap \Omega$. If the flow is smooth and the matrix whose columns are the tangent vectors $u^i_{,t}$ and $u^i_{,\sigma_j}$ is full rank (k) for all $|t| < T$,$\sigma \in \Omega_\sigma$), then because the trajectories are smooth in the intial conditions, the surface is well defined and is indeed a manifold.

Hale [14] calls these *integral manifolds*, and seems to reserve *invariant manifold* for the stable and unstable manifolds of fixed points and periodic motions.

†IBM Research Division, T. J. Watson Research Center, Yorktown Heights, NY 10598, mhender@watson.ibm.com

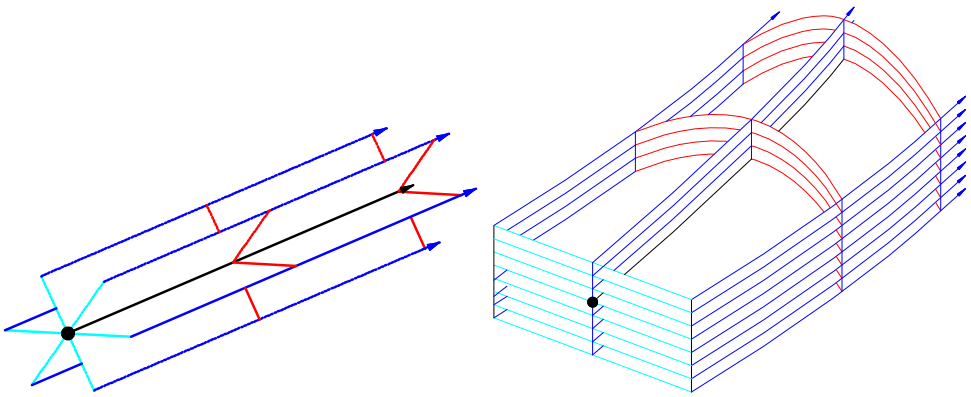

FIG. 1.1. *It is not possible to decide if a point lies on a particular invariant manifold. A point lies on a unique 1d invariant manifold (a trajectory), but there is a continuum of higher dimensional manifolds containing the trajectory (left). Another way of saying this is that near any particular invariant manifold there is a set of parallel manifolds which cover the entire phase space (right).*

Certain nontrivial, globally well defined invariant manifolds can exist in a flow. These include fixed points ($k = 0$), periodic orbits ($k = 1$), and invariant tori ($k = 2$). By globally well defined we mean that the manifold of starting points is uniquely defined up to an infinitesimal translation in the direction of the tangent space of the manifold. For periodic orbits the tangent space is one dimensional and the translation is a phase shift. Adding a phase constraint determines $\mathbf{c}$, which can be computed directly (a shooting method), or a system can be written for the entire manifold. This second approach has been used for invariant tori by Dieci and Lorenz [6] and Moore [27].

Other global invariant manifolds include the stable and unstable manifolds of a hyperbolic fixed point $\mathbf{u}_0$ –

$$W^s(\mathbf{u}_0) = \{\mathbf{u} \mid \lim_{t\to\infty} \phi_F^t(\mathbf{u}) = \mathbf{u}_0\}$$
$$W^u(\mathbf{u}_0) = \{\mathbf{u} \mid \lim_{t\to-\infty} \phi_F^t(\mathbf{u}) = \mathbf{u}_0\},$$

and the the stable an unstable manifolds of hyperbolic periodic orbits. These manifolds provide significant insight into the structure of chaotic attractors (see in particular Abraham and Shaw [1], and Jackson [18], [19]). Asymptotic expansions for the stable and unstable manifolds of a hyperbolic fixed point can be found near the fixed point [3], [29], Appendix C: tangent to the eigenspaces of the Jacobian F_u at the fixed point with negative and positive real parts respectively. These expansions, together with the condition that the projection of $\mathbf{c}(\sigma)$ onto the eigenspace is a small sphere, defines $\mathbf{c}(\sigma)$.

In the visualization of steady fluid flows, which are two or three dimensional dynamical systems, the invariant manifold associated with a curve (called a *rake*) is called a stream surface, and a trajectory is stream line. Algorithms are available for finding a set of stream lines which covers the phase space, [33], [34], [17]. Stream surfaces from carefully placed initial curves are useful in experiments for visualizing the flow (e.g [25], [2]), This can be done by injecting smoke or dye into the flow from holes spaced along a thin tube – which trace streamlines which look something like the tracks of a rake through sand. Another technique (the "smoke-wire" technique) usses a current to heat a wire which is covered with oil. This generates an invariant

manifold of smoke, with the wire being the manifold of starting points.

Recent work in orbital mechanics suggests that invariant manifolds may be used to construct spacecraft missions with low fuel requirements. An invariant manifold gives the set of points that can be reached from a manifold of starting points with no expenditure of fuel (ideally). Low fuel space missions can therefore be constructed by finding where invariant manifolds intersect certain objectives, and using small amounts of fuel to move to the corresponding starting point. See Marsden et. al. [10], Howell et. al. [16].

Invariant manifolds are not locally defined. That is, it doesn't make sense to ask which invariant manifold a point lies on, nor is there a local test to determine if a point lies on the manifold generated by a particular initial curve. A point lies on a continuum of invariant manifolds, whose intersection is the trajectory through the point (Figure 1.1), or equivalently, near every invariant manifold lies a parallel family of invariant manifolds (if $k < n$) which cannot be distinguished locally. Computationally, this means that a local method that drifts off the manifold has no way to move back to the manifold without returning to $\mathbf{c}(\sigma)$. In addition, the parameterization $\mathbf{u}(t, \sigma)$ is extremely poor in most interesting examples.

The method presented here generates a uniform distribution of points on the manifold, most of which lie on trajectories. These trajectories start either at a point on $\mathbf{c}(\sigma)$ or at an interpolation point. Two interpolation methods are suggested, one which interpolates from adjacent trajectories, the other solves a two point boundary value problem to find an interpolation point on a trajectory starting on $\mathbf{c}(\sigma)$.

We begin in Section 2 with a review of tensor notation and concepts from differential geometry. In section 3 we review several recently proposed methods of computing invariant manifolds, and characterize them by how the invariant manifold is parameterized. In Section 4 we describe our method for computing a "fat" trajectory, which uses small coordinate patches on the invariant manifold along a trajectory to cover the trajectory with a uniform distribution of points.

In Section 5 we use the algorithm to compute the stable manifold of the origin in the Lorenz system.

In Appendices A, B and C we present the main theoretical results of this paper: how to find orthonormal coordinate patches along a trajectory, how to choose interpolation points, and a result giving a manifold of starting points for computing the stable or unstable manifold of a fixed point.

2. Metrics, Connections and Curvature Tensors. The algebra below involves the "usual" tensors that arise in differential geometry. Therefore we use tensor notation throughout. The reader may find a good description in the books of Eisenhart [9], Lovelock and Rund [26], and Spivak vol. 2 [31]. A quick review, to establish notation –

Vectors – A vector $\mathbf{u} \in \mathbb{R}^n$ will be written as u^i, which are the coordinates of $\mathbf{u}$ in some coordinate system.

Differentiation – The partial derivatives of a vector valued function $u^i(s)$, $s \in \mathbb{R}^k$ will be written $u^i_{,j}$ which stands for $\partial u^i / \partial s^j$. The "comma" indicates the differentiation, $j \in [0, k)$

The summation convention – A repeated subscript indicates a sum over the range of the index, so that $u^i_{,j} s^j = \sum_j u^i_{,j} s^j$.

With the summation convention a Taylor series for $\mathbf{u}(\mathbf{s})$ to third order can be written compactly as

$$u^i(\mathbf{s}) \sim u^i + u^i_{,j} s^j + \frac{1}{2} u^i_{,j,k} s^j s^k + \frac{1}{6} u^i_{,j,k,l} s^j s^k s^k$$

We will be dealing with k dimensional manifolds embedded in n space, which in some neighborhood of a point u^i can be expressed as an n-vector valued function of a k-vector: $u^i(\mathbf{s})$. The parameterization determines a basis for the tangent space of the surface at any point $\mathbf{s}$,

$$\phi_j = \left(\frac{\partial u^0}{\partial s^j}, \frac{\partial u^1}{\partial s^j}, ..., \frac{\partial u^{n-1}}{\partial s^j} \right) = u^i_{,j}$$

This is the tangent to the j^{th} coordinate line – the curve obtained by varying only the j^{th} coordinate of $\mathbf{s}$.

We will also occasionally refer to a basis for the orthogonal complement in $\mathbb{R}^n$ of the k-dimensional tangent space, and will call this v^i_j. We will assume that it is orthonormal, so that

$$u^p_{,i} v^p_j = 0 \qquad \text{and} \qquad v^p_i v^p_j = \delta_{ij}.$$

With this notation we can define the basic concepts from differential geometry –

The metric g_{ij} – the matrix of inner products of the basis vectors

$$g_{ij} = u^p_{,i} u^p_{,j}$$

For a Euclidean metric, (an orthonormal basis) $g_{ij} = \delta_{ij}$. The inverse of the metric is usually written g^{ij}

$$g^{ip} g_{pj} = \delta^i_j \qquad\qquad g_{ip} g^{pj} = \delta^j_i$$

The connection Γ_{ijk} **and** η_{ijk} **(Christoffel symbols of the** 1^{st} **kind)** – are the inner products of the basis vectors and the second derivatives

$$\Gamma_{ijk} = u^p_{,i} u^p_{,j,k} \qquad\qquad \eta_{ijk} = v^p_{,i} u^p_{,j,k}$$

These are the projections of the second derivatives of the surface into the two bases, and can be used to reconstruct the second derivatives

$$u^i_{,j,k} = \Gamma^p_{jk} u^i_{,p} + \eta^p_{jk} v^i_p$$

$$\Gamma_{ijk} = u^p_i u^p_{,j,k} = \Gamma^p_{jk} g_{ip}, \qquad \eta_{ijk} = v^p_i u^p_{,j,k} = \eta^p_{jk} \delta_{ip}$$

The symbols Γ^i_{jk} and η^i_{jk} are called the Christoffel symbols of the 2^{nd} kind.

The curvatures Γ_{ijkl} **and** η_{ijkl} – By analogy with the connection, we can define the inner products

$$\Gamma_{ijkl} = u^p_{,i} u^p_{,j,k,l} \qquad\qquad \eta_{ijkl} = v^p_{,i} u^p_{,j,k,l}$$

And reconstruct the third derivatives

$$u^i_{,j,k,l} = \Gamma^p_{jkl} u^i_{,p} + \eta^p_{jkl} v^i_p$$

$$\Gamma_{ijkl} = u^p_i u^p_{,j,k,l} = \Gamma^p_{jkl} g_{ip}, \qquad \eta_{ijkl} = v^p_i u^p_{,j,k,l} = \eta^p_{jkl} \delta_{ip}$$

The symbols are useful to us in part because they give a Taylor series for the surface. (Higher order symbols can be defined in the same way.)

$$u^i(s) \sim u^i + u^i_{,p} s^p + \tfrac{1}{2}\left(\Gamma^p_{jk} u^i_{,p} + \eta^p_{jk} v^i_p\right) s^j s^k + \tfrac{1}{6}\left(\Gamma^p_{jkl} u^i_{,p} + \eta^p_{jkl} v^i_p\right) s^j s^k s^l$$

$$= u^i + \left(s^p + \tfrac{1}{2}\Gamma^p_{jk} s^j s^k + \tfrac{1}{6}\Gamma^p_{jkl} s^j s^k s^l + ...\right) u^i_{,p}$$

$$+ \left(\quad \tfrac{1}{2}\eta^p_{jk} s^j s^k + \tfrac{1}{6}\eta^p_{jkl} s^j s^k s^l + ...\right) v^i_p$$

The Γ's control the parameterization in the tangent space, while the η's define the surface.

Eq. 1.1 gives a parameterization derived from $\mathbf{c}(\sigma)$ and the dynamics. If we change the parameterization in the tangent space and transform the η's accordingly, we can replace this poor parameterization yet preserve the manifold.

Note that the connection can also be defined in terms of derivatives of the metric (this is the more usual definition)

$$\Gamma_{ijk} = u^p_{,i} u^p_{,j,k} = \quad \frac{1}{2}\left((u^p_{,i} u^p_{,j})_{,k} + (u^p_{,i} u^p_{,k})_{,j} - (u^p_{,j} u^p_{,k})_{,i}\right)$$

$$= \quad \frac{1}{2}\left(\frac{\partial g_{ij}}{\partial s^k} + \frac{\partial g_{ik}}{\partial s^j} - \frac{\partial g_{jk}}{\partial s^i}\right)$$

and a similar expression exists for the third derivatives

$$(g_{ij})_{,k} \quad = \Gamma_{ijk} + \Gamma_{jik}$$

$$(\Gamma_{ijk})_{,l} \quad = u^p_{,i} u^p_{,j,k,l} + u^p_{,i,l} u^p_{,j,k}$$

$$= \Gamma_{ijkl} + g_{qr}\Gamma^q_{il}\Gamma^r_{jk} + \delta_{qr}\eta^q_{il}\eta^r_{jk}.$$

So

$$\Gamma_{ijkl} = (\Gamma_{ijk})_{,l} - \Gamma_{pil}\Gamma^p_{jk} - \eta_{pil}\eta^p_{jk},$$

which will be useful later, and indicates the relation to the Riemannian curvature tensor $R_{ijkl} = \Gamma_{ijkl} - \Gamma_{ijlk}$.

3. Basic Ideas and Approaches. For finite time the initial value problem is smooth in the initial conditions, so if $\mathbf{c}(\sigma)$ is smooth, and transverse to the flow, $M_{\mathbf{c}}$ will be smooth (for finite time). Points at which $\mathbf{c}(\sigma)$ is tangent to the flow do not define a full neighborhood of initial conditions, and generate a boundary of $M_{\mathbf{c}}$. The parameterization (t, σ) will doubly cover a neighborhood of $M_{\mathbf{c}}$ near such points.

Following Hultquist's terminology [17], we call the image of a simplex on $\mathbf{c}(\sigma)$ a *ribbon*. A *front*, which is the image of the initial curve at some fixed time (Figure 3.1). Fronts may become stretched as time increases, but remain smooth and transverse to the flow for finite time if $\mathbf{c}$ is smooth and transverse.

In principle the integral Eq. (1.1) is sufficient to compute the invariant manifold. We have an explicit parameterization of the invariant manifold, and can compute points on a regular mesh on the manifold by solving initial value problems for a regular mesh of initial conditions on $\mathbf{u}(0, \sigma)$. If the mesh is fine enough we can find

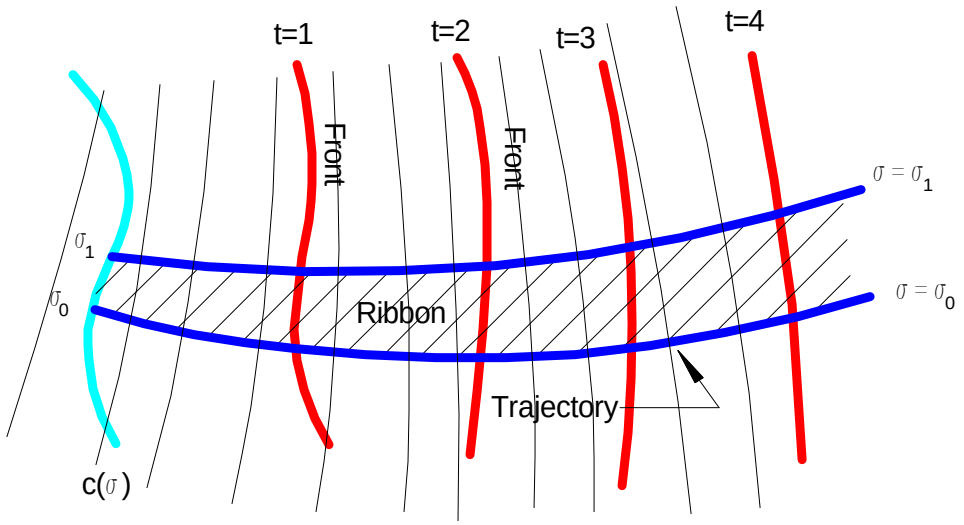

FIG. 3.1. *Fronts (red, images of the initial curve under the flow) and ribbons (the shaded area between the two blue trajectories). The black curves are fronts which are locally orthogonal to the trajectories, whose existance is the subject of the flow box theorem.*

points so that some finite part of the manifold (e.g. $0 \leq t \leq T$) is sampled to any desired density. However, this parameterization often proves to be very poor. Figure 3.2 shows a 2d sketch of the typical problems. In Figure 3.2a a very fine mesh is needed on $\mathbf{u}(0, \sigma)$ to obtain an adequate mesh on $\mathbf{u}(T, \sigma)$. In 3.2b mesh cells are drastically sheared. And of course, either situation may occur at different points along $\mathbf{u}(0, \sigma)$.

The quality of a parameterization can be measured by how close the metric (the matrix of inner products of the tangent vectors) is to the identity. The determinant of the metric is the ratio of the volume of the image of a small cube in parameter space to the volume of the cube. In a good parameterization the metric is everywhere close to the identity, which means that the coordinate system is locally almost orthonormal. In 3.2a the metric is nearly diagonal, but the diagonal elements are large. In 3.2b the off diagonal terms of the metric are large relative to the diagonal elements.

A reparameterization chooses new coordinates, $\mathbf{s}(t, \sigma) \in \mathbb{R}^k$ for the invariant manifold. This may be done explicitly, implicitly, or by remeshing. A mesh is a discrete representation of the inverse of the mapping $\mathbf{s}(t, \sigma) \in \mathbb{R}^k$, the vertices of the mesh being points (t_i, σ_i). For a one dimensional mesh this is easily seen, since the labelling of the mesh points s_i is an explicit mapping from a uniform mesh on part of the real line. The quality of the mesh can be measured by the norm of the linear map from each mesh cell to a standard mesh cell.

Scaling time changes the parameterization of the trajectories, but not the trajectories themselves. If $u^i(t)$ is a trajectory of $u^i_{,t}(t) = F^i(\mathbf{u}(t))$, then $u^i(t(\tau))$ is a trajectory of $u^i_{,t}(t(\tau)) = F^i(\mathbf{u})/t_{,\tau}(\tau)$. Therefore, the magnitude of $\mathbf{F}$ does not effect the manifold, but does change the shape of the fronts. The Flow Box theorem implies that near a ribbon time can be scaled to give a set of fronts which are orthogonal to the ribbon (see Figure 3.1). This cannot be done globally. If the metric is block diagonal, scaling time, together with an independant scaling of σ is sufficient. This does not however, improve the sheared case shown in Fig. 3.2b, where the flow becomes almost tangential to the front and the off–diagonal terms in the metric are large.

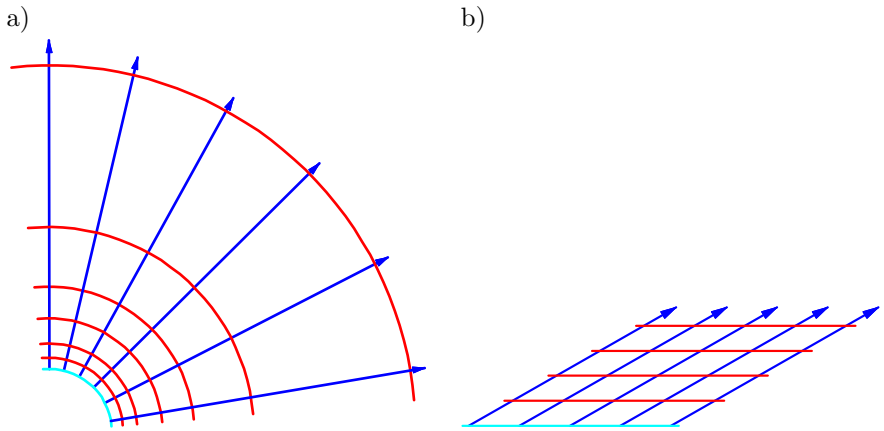

FIG. 3.2. *Typical problems with the global parameterization. a) The metric is nearly diagonal, but the diagonal elements are large. b) The off-diagonal elements are the same order of magnitude as the diagonal elements. Both cases imply that a uniform mesh on the initial manifold (with metric the identity) will in time result in a poor distribution of points on the manifold. In each case the fronts (red) and ribbons (bounded by the blue trajectories) are shown.*

We now turn to existing methods for computing invariant manifolds. Three of these rescale t and σ separately, and three use non-diagonal scalings. While the method proposed here is derived independantly, it incorporates the basic ideas of several of these methods.

Hultquist [17] scales time by using $\mathbf{F}/|\mathbf{F}|$ instead of $\mathbf{F}$, and scales σ by splitting and joining ribbons, so that the size of mesh cells on a front are controlled.

$$\mathbf{u}_H(t_{i+1},\sigma_j) - \mathbf{u}_H(t_i,\sigma_j) = \int_{t_i}^{t_{i+1}} \mathbf{F}(\mathbf{u}_H(\tau,\sigma_j))(F^pF^p)^{-1/2}\mathrm{d}\tau$$

$$.5\Delta \le |\mathbf{u}_H(t_i,\sigma_{j+1}) - \mathbf{u}_H(t_i,\sigma_j)| \le \Delta$$

If the distance between consequetive points on the front exceeds the threshold, a new point is interpolated in between. If points are too close together, one is deleted. The first constraint approximates $|(\mathbf{u}_H)_{,t}| = 1$, and the second approximates $.5 \le |(\mathbf{u}_H)_{,\sigma}| \le 1$.

Johnson, Jolly and Kevrekidis (JJK) [20] scale time by using $\mathbf{F}/\sqrt{|\mathbf{F}|^2+1}$ instead of $\mathbf{F}$, and redistribute points along each front so that the mesh cells are of equal size.

$$\mathbf{u}_{JJK}(t_{i+1},\sigma_j) - \mathbf{u}_{JJK}(t_i,\sigma_j) = \int_{t_i}^{t_{i+1}} \mathbf{F}(\mathbf{u}_{JJK}(\tau,\sigma_j))(1+F^pF^p)^{-1/2}\mathrm{d}\tau$$

$$|\mathbf{u}_{JJK}(t_i,\bar\sigma_{j+1}) - \mathbf{u}_{JJK}(t_i,\bar\sigma_j)| = \Delta$$

Here $\sigma_j \le \bar\sigma_{j'} \le \sigma_{j+1}$, and $\mathbf{u}_{JJK}(t_i,\bar\sigma_j)$ is interpolated from $\mathbf{u}_{JJK}$ at those points. The first constraint approximates $|(\mathbf{u}_H)_{,t}| = 1$, and the second $|(\mathbf{u}_H)_{,\sigma}| = 1$.

Doedel [7] scales time by distributing mesh points along the trajectory (using a boundary value solver), and uses an implicit scaling for σ, requiring that ribbons

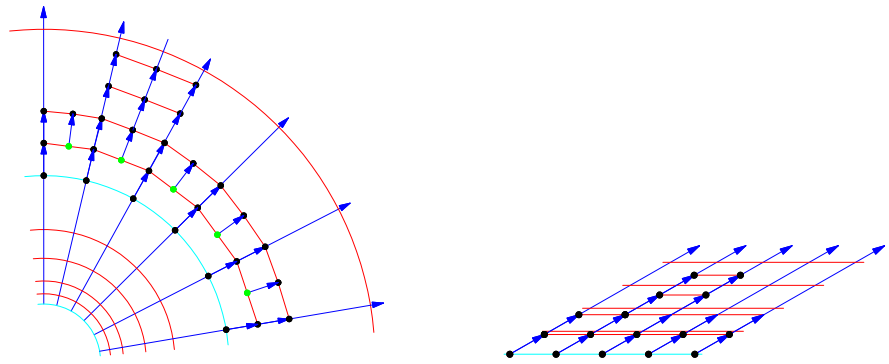

a) Hultquist

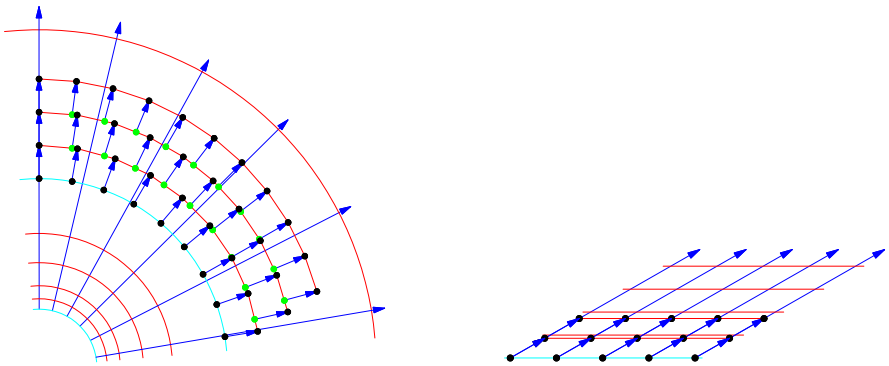

b) Johnson, Jolly and Kevrekedis

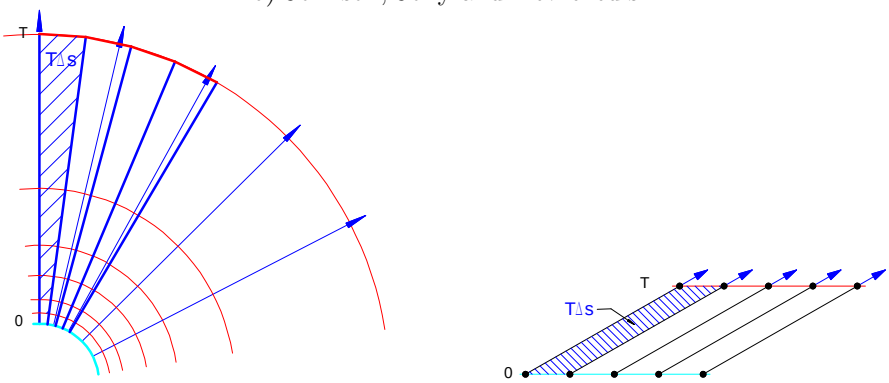

c) Doedel

FIG. 3.3. *A sketch of the first three methods, which use diagonal scalings, for comparison. Interpolation points are indicated in green, the manifold of starting points in cyan, and the fronts and ribbons in blue and red. All work well when the metric is poorly scaled but diagonal, and as expected, not as well in the non-diagonal case. Note that Doedel's method needs no interpolation, and that Johnson, Jolly and Kevrekedis' method interpolates almost every point.*

have equal areas.

$$\begin{aligned}
&\mathbf{u}'_D(t,\sigma_j) = \mathbf{F}(\mathbf{u}_D(t,\sigma_j)) \\
&\mathbf{u}_D(0,\sigma_j) = \mathbf{c}(\sigma_j) \\
&0 \le t \le T
\end{aligned}$$

$$\frac{1}{T\Delta}\int_0^T (u_D^p)_{,\sigma}(\tau,\sigma_j)(u_D^p(\mathfrak{s},\sigma_{j+1})) - u_D^p(\tau,\sigma_j)\mathrm{d}\tau = 1$$

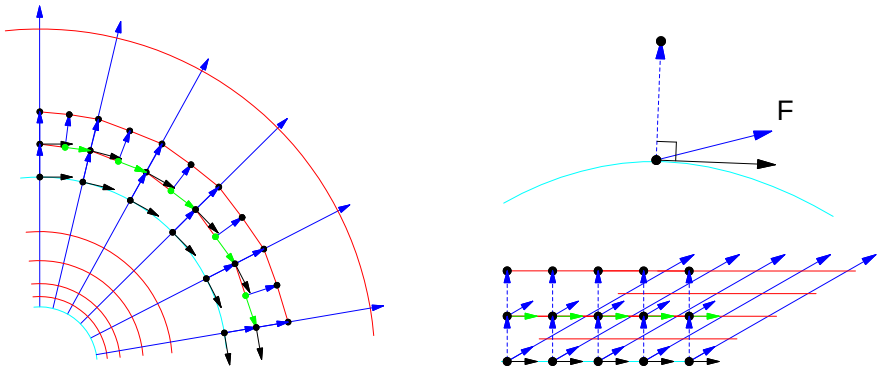

d) Guckenheimer and Worfolk

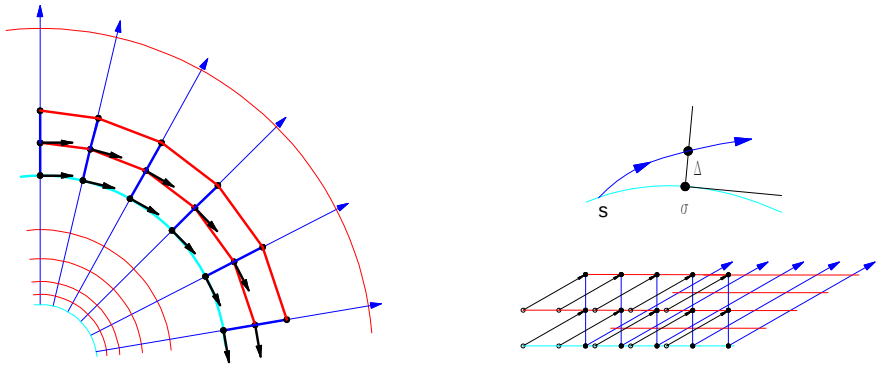

e) Krauskopf and Osinga

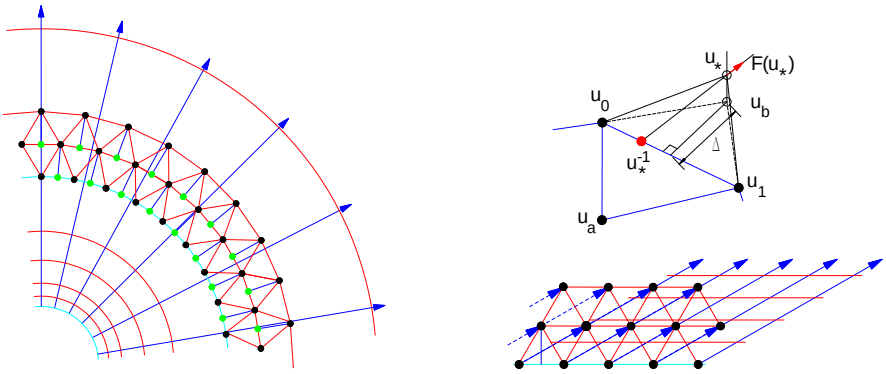

f) Guckenheimer and Vladimirsky

FIG. 3.4. *A sketch of the second three methods, which use non-diagonal scalings, for comparison. All three deal with both poor diagonal and non-diagonal metrics, but differ in the number and quality of interpolations.*

This constraint is an approximation of $\frac{1}{T}\int_0^T |(\mathbf{u}_D)_{,\sigma}|^2 \mathrm{d}t = 1$.

The remaining three algorithms all use upper block triagonal scalings.

Guckenheimer and Worfolk [13] diagonalize the metric by replacing t with a new parameter τ which is a linear combination of t and σ, so that $\mathbf{u}_{,\tau} = \alpha_t \mathbf{u}_{,t} + \alpha_{\sigma_j} \mathbf{u}_{,\sigma_j}$

is orthogonal to $\mathbf{u}_{,\sigma_j}$. See Figure 3.4.

$$(\mathbf{u}_{GW})_{,\tau}(t_i,\sigma_j) = \alpha_t \mathbf{F}(\mathbf{u}_{GW}(t_i,\sigma_j)) + \alpha_\sigma (\mathbf{u}_{GW})_{,\sigma}(t_i,\sigma_j)$$

$$|(\mathbf{u}_{GW})_{,\tau}(t_i,\sigma_{j+1})| = 1$$

$$(u^p_{GW})_{,\tau}(t_i,\sigma_j)(u^p_{GW})_{,\sigma}(t_i,\sigma_j) = 0$$

To find $\mathbf{u}_{,\tau}$ the tangents $\mathbf{u}_{,\sigma}$ must be known, so only one time step can be taken between fronts, and the $\mathbf{u}_{,\sigma}$ must be estimated (interpolated) at each point on the new front. The second and third constraints require that τ is unit length, and orthogonal to the σ direction.

Krauskopf and Osinga [21], [22], [23] also replace time with an implicit combination of t and σ, and scale σ by splitting and merging ribbons. They use an integral version of the differential constraint used by Guckenheimer and Worfolk .

$$u^i_{KO}(t_{i+1},\sigma_j) = u^i_{KO}(t_i,\sigma_j) + \int_{t_i}^{t_{i+1}} F^i(\mathbf{u}_{KO}(\tau,s_j))\mathrm{d}\tau$$

where s_j is chosen so that

$$|\mathbf{u}_{KO}(t_{i+1},\sigma) - \mathbf{u}_{KO}(t_i,\sigma_j))| = \Delta$$

$$(u^p_{KO})_{,\sigma_j}(t_i,\sigma_j)(u^p_{KO}(t_{i+1},\sigma_j) - u^p_{KO}(t_i,\sigma_j)) = 0$$

The first constraint approximates $|(\mathbf{u}_H)_{,t}| = 1$, and the second requires that the t direction is orthogonal to the σ direction.

Guckenheimer and Vladmirisky [12] represent the manifold with a triangulation, whose boundary is a polygonal curve. A point on a boundary edge is advanced using a one step backward Euler scheme. The parameterization is determined by requiring that the projection of the new point $\mathbf{u}_*$ onto the plane defined by the triangle opposite the boundary edge be a particular distance from the edge. That is, if the triangle opposite the boundary edge $\mathbf{u}_0 \leftrightarrow \mathbf{u}_1$ is $\Delta\mathbf{u}_0\mathbf{u}_1\mathbf{u}_a$, and $\mathbf{u}_b$ is a point in the same plane as this triangle, on the opposite side of the edge being advanced, then the advanced point $\mathbf{u}_*$ satisfies

$$\begin{aligned}
&\mathbf{u}_* - \frac{\beta_0\mathbf{u}_0 + \beta_1\mathbf{u}_1}{\beta_0+\beta_1} = \frac{\mathbf{F}(\mathbf{u}_*)}{\beta_0+\beta_1}\\
&(\mathbf{u}_0 - \mathbf{u}_a).(\mathbf{u}_* - \mathbf{u}_b) = 0\\
&(\mathbf{u}_1 - \mathbf{u}_a).(\mathbf{u}_* - \mathbf{u}_b) = 0
\end{aligned}$$

This is a set of $(n+2)$ equations for the $(n+2)$ unknowns $(\mathbf{u}_*, \beta_0, \beta_1)$, and it's generalization to higher dimensions is straightforward when written in this form. The tangent plane at the new point has two components: one along the flow $\mathbf{F}$, and the other the edge $\mathbf{u}_0 \leftrightarrow \mathbf{u}_1$. By analogy with the convection of fluid properties, an upwinding constraint should be applied, which is that $\mathbf{u}_*^{-1}$ lie between $\mathbf{u}_0$ and $\mathbf{u}_1$. This is exactly the condition that the β's be non-negative. Guckenheimer and Vladimirsky suggest ordering the boundary edges and advancing the edge which is most "upwind".

4. Covering an invariant manifold with fat trajectories. Two basic types of errors committed by these algorithms: one in advancing a point along a trajectory,

and the other in interpolating a new point on the manifold. The error committed in moving along a trajectory is related to the error in the starting point on $\mathcal{S}_i$, the length of the integration, and the stability of the trajectory. A stable integration scheme can integrate a trajectory on an invariant manifold which is not attracting in the normal direction, and the total error can be controlled. However, an error in the initial point normal to the manifold will still be amplified when the manifold is not attracting in the normal direction. This initial error comes from interpolating a point on the manifold (unless the trajectory starts on the manifold of starting points). This error is usually controlled by the spacing of points on $\mathbf{c}(\sigma)$, and the criteria for inserting points on the new front.

4.1. Constructing a covering . Instead of explicitly reparameterizing, we look for a uniform distribution of points on the invariant manifold, using the algorithm described in [15]. This begins with a single point $\mathbf{u}_0$ on the manifold, a k-dimensional spherical ball $B_{R_0}(0)$ in the tangent space at $\mathbf{u}_0$, and a k-dimensional convex polyhedron P_0 which contains the ball. At each step we have a set of points $\mathbf{u}_i$, balls $B_{R_i}(0)$ and polyhedra P_i. The union of the balls (or rather, the projection of the balls from the tangent space at $\mathbf{u}_i$ onto the manifold) is the set of points on the manifold that are close to the $\mathbf{u}_i$.

At each step we choose a new point on the boundary of the union of balls (see below). This ensures that the points are well distributed. For any $i > j$, $\mathbf{u}_i$ must be outside the ball about $\mathbf{u}_j$, so the radius of the balls determines the minimum allowed distance between points. Also, a ball is either on the boundary, or each point on the sphere about the point is interior to another ball (so the centers aren't too far apart).

If the ball about a new point $\mathbf{u}_m$ overlaps the ball about $\mathbf{u}_j$, half spaces are subtracted off P_m and P_j. Let Φ_m^* be the projection from $\mathbb{R}^n$ onto the tangent space of the invariant manifold at $\mathbf{u}_m$. (If the basis for the tangent space at $\mathbf{u}_m$ is orthonormal Φ_m is the matrix whose columns are the basis vectors.) If $s_{mj} = \Phi_m^*(\mathbf{u}_j - \mathbf{u}_m)$, then the intersection of the spheres $\delta B_{R_m}(0)$ and $\delta B_{R_j}(s_{mj})$ lies in a plane orthogonal to the line from the origin to s_{mj} and contains the point $\alpha_{mj} s_{mj}$ where $\alpha_{mj} = (1 + (R_m^2 - R_j^2)/|s_{mj}|^2)/2$. The half space removed from P_m is the set of points $\left\{ s \mid s.s_{mj} > \alpha_{mj} |s_{mj}|^2 \right\}$. The same procedure is used to subtract a half space from P_j with j and m interchanged in the above expressions. See Figure 4.1.

Points on the boundary of the union of balls can be found in terms of the vertices of the polyhedra. If P_i has a vertex with radius greater than R_i, that ball lies on the boundary (and the part of the sphere inside the polyhedra is that part that lies on the boundary). If all the vertices are inside the ball, that ball is interior to the union. Of course, this gives a point in the tangent plane at $\mathbf{u}_i$, not on the manifold. We refer the reader to [15] for details about the balls and polytopes.

4.2. Generating points on the invariant manifold using fat trajectories. We will cover the invariant manifold by computing ribbons. We use a trajectory as the centerline of the ribbon and a second order approximation to the invariant manifold at each point on the trajectory to define the edges. That is, we compute $(u^i, u^i_{,j}, u^i_{,j,k})$, at each point on the trajectory with the understanding that

$$u^i(\mathbf{s}) \sim u^i + u^i_{,j} s^j + \frac{1}{2} u^i_{,j,k} s^j s^k,$$

and define the ribbon to be $\left\{ \mathbf{u} \in M_{\mathbf{c}} \mid \mathbf{u} = \mathbf{u}_i(s),\ |\mathbf{u}_{,j,k} s^j s^k| \leq 2\epsilon \right\}$.

In Appendix A we derive evolution equations in scaled time τ, for such an approximation in a locally Euclidean coordinate system, and show how to find an initial

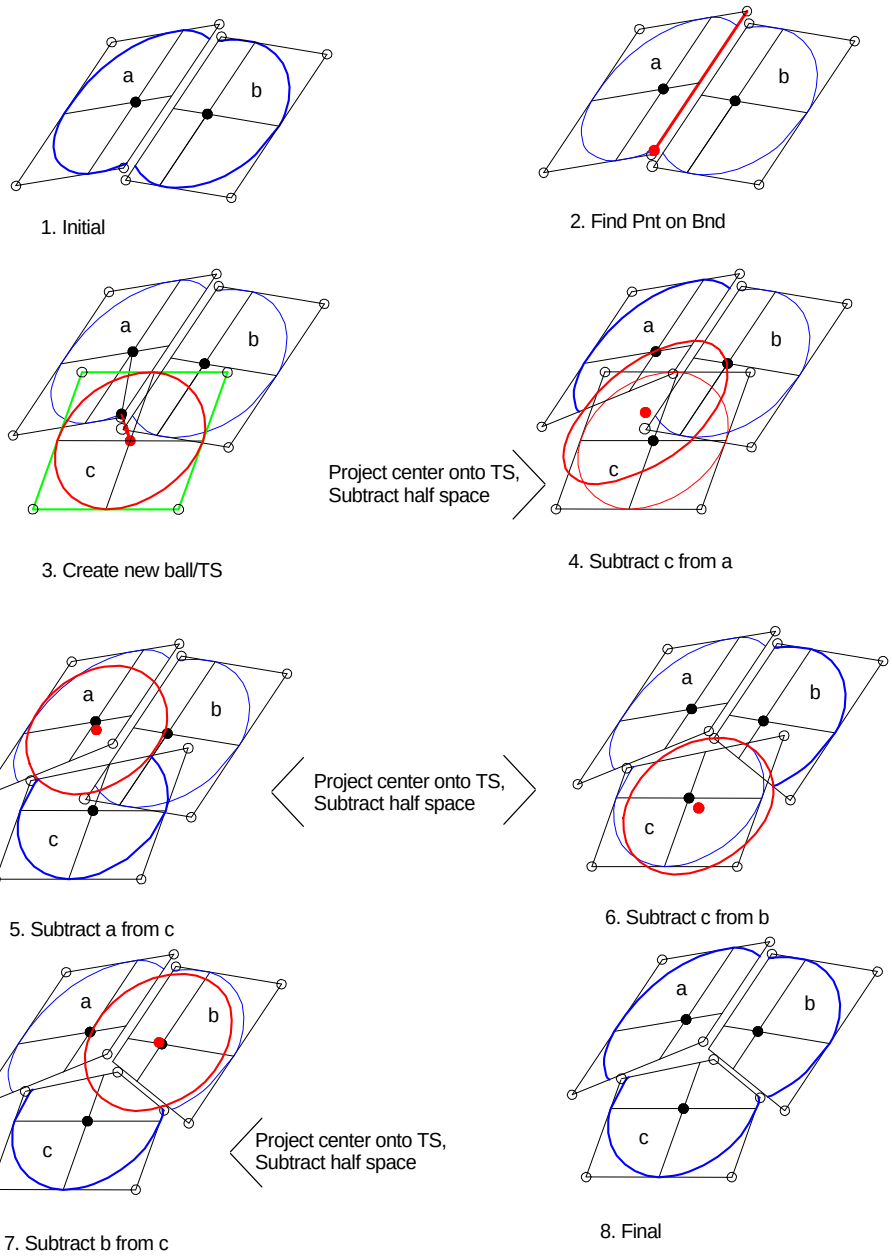

FIG. 4.1. *The basic steps in the continuation. k inner products of n vectors are needed to project into a tangent space, some way of projecting a point down onto the manifold must be provided.*

approximation at points on $\mathbf{c}(\sigma)$. The evolution equations are

$$u^i_{,\tau} = (F^w F^w)^{-1/2} F^i$$

$$u^i_{,\tau,j} = (F^w F^w)^{-1/2} \left(F^i_{,p} u^p_{,j} - u^p_{,r} F^p_{,q} u^q_{,j} u^i_{,r} \right)$$

$$u^i_{,\tau,j,k} = (F^w F^w)^{-1/2} \left(F^i_{,p} u^p_{,j,k} + F^i_{,p,q} u^p_{,j} u^q_{,k} - u^p_{,r} F^p_{,q} u^q_{,j} u^i_{,r,k} - u^p_{,r} F^p_{,q} u^q_{,k} u^i_{,j,r} \right)$$

$$-(F^w F^w)^{-1/2} \left(u^p_{,r} F^p_{,q} u^q_{,j,k} + u^p_{,r} F^p_{,q,v} u^q_{,j} u^v_{,k} + u^p_{,j,k} F^p_{q} u^q_{,r} \right) u^i_{,r}$$

This means that points on the ribbon can be computed using an initial value solver for a larger system of equations. We call this ribbon a "fat trajectory".

Figure 4.2 shows a sequence of approximations along a trajectory, the union of balls at these points on the ribbon, and the polyhedra used to find the boundary of the union. If the distance between points $\mathbf{u}_i$ and $\mathbf{u}_{i+1}$ on the trajectory is R_i, $\mathbf{u}_{i+1}$ is on the boundary of the union of the previous balls on the ribbon. The width of the ribbon defines $R \sim \sqrt{2\epsilon/A}$, where A is the norm of the second derivative terms.

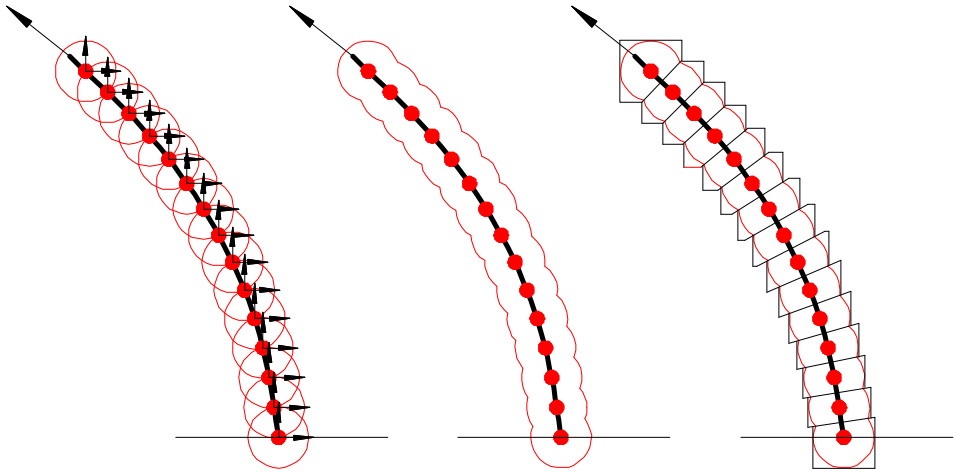

FIG. 4.2. *A fat trajectory used as a ribbon. Left: points along the trajectory with local expansions inside balls. (Note that the coordinate systems for the expansions are not aligned with the trajectory and are orthonormal.) Middle: the union of the balls, which is the ribbon. Right: the polyhedron used to represent the boundary of the union.*

Note that the trajectory at the center of the ribbon may pass close to itself, or it may pass close to another ribbon. In this case the point at the advancing end of the ribbon may lie inside one of the other balls. This is easily tested, since to add a new point we must find all nearby balls (a set of hierarchical bounding boxes may be used, so this does not require checking all other balls), and the nearby balls can be checked. If the new point is interior to any of the balls the point is not added, and we continue following the ribbon until a new point is found that is exterior.

4.3. Interpolating to start new fat trajectories . We select a point on $\mathbf{c}(\sigma)$, and integrate the fat trajectory containing it forward in time a distance T (or until the trajectory leaves Ω). Then choose a new point on $\mathbf{c}(\sigma)$ that is outside the other balls to start a new fat trajectory and repeat until $\mathbf{c}(\sigma)$ is covered. When we finish these initial fat trajectories we have a set of points $\{\mathbf{u}_i \in M_{\mathbf{c}}\}$ which lie along trajectories, and balls in the tangent space of $M_{\mathbf{c}}$, $B_{R_i}(0) \in TM_{\mathbf{c}}$. (See Figure 4.3.) These points will not, in general, cover all of $M_{\mathbf{c}}$.

To proceed we want to choose a point near the boundary of the projection of these balls onto the manifold, at which the flow is outward from the boundary. This ensures that the new fat trajectory covers part of $M_{\mathbf{c}}$ that is as yet uncovered. We also need to find an approximation of the derivatives of the manifold to use as initial conditions for the fat trajectory. We might expect that points closer to the initial curve are better than points further away, and this does indeed lead to a good choice of interpolation point, and ensures that $M_{\mathbf{c}}$ is completely covered.

We define something like a constrained optimization problem on the invariant manifold, and choose the "minimizer" of this problem as an interpolation point. Points on $M_{\mathbf{c}}$ are allowed to move backward under the flow toward $\mathbf{c}(\sigma)$, but not allowed to cross into the union of the balls (Figure 4.3). In Appendix B we show that a point $\mathbf{u}_*$ exists which is stationary under this procedure, and that $\mathbf{u}_*$ lies on the intersection of k spheres, where a line parallel to $\mathbf{F}$ through $\mathbf{u}_*$ intersects the simplex formed by the centers of the intersecting balls at an interior point $\tilde{\mathbf{u}}_*$. If the variation of $\mathbf{F}$ over a single ball is small, a trajectory starting at $\tilde{\mathbf{u}}_*$ will leave the interior of the union of balls near $\mathbf{u}_*$ Values can be interpolated from the values at the centers of the balls for starting a fat trajectory at $\tilde{\mathbf{u}}_*$. (Figures 4.5 and 4.6.)

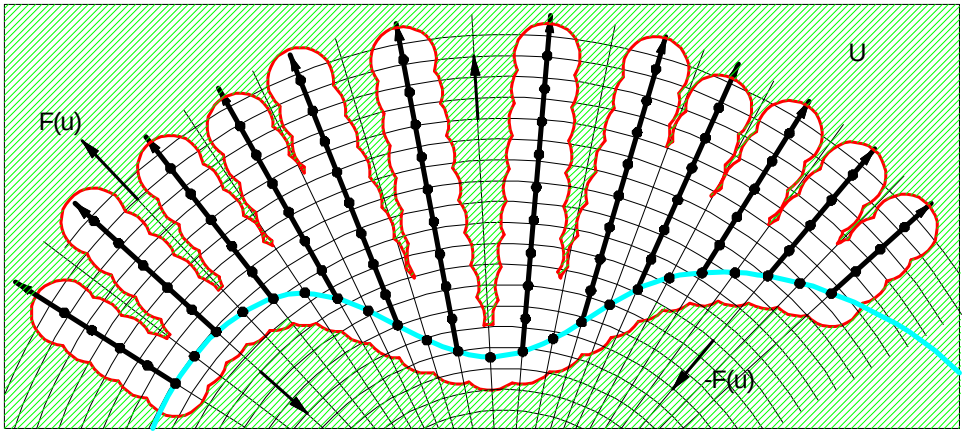

FIG. 4.3. *A continuation after integrating fat trajectories starting from a series of points on the manifold of starting points (every other point in this case). An optimization problem is posed in U – the complement of the interior of the balls on the invariant manifold M. Each point on M integrates backward or forward in time to the manifold of starting points, and we move each point in U in this direction until the surface of the balls is encountered. At that point the flow induced on the surface by projecting into the tangent space is used.*

The points where k spheres intersect are points where an edge of the polyhedron associated with a ball cross the ball (this is true for any k). The edges and their endpoints are stored for updating the polyhedra, and if the endpoints of a candidate edge are $\mathbf{v}_0$ and $\mathbf{v}_1$ (in the coordinate system on the tangent space), the edge intersects the ball of radius R centered at the origin iff

$$|\mathbf{v}_0 + t_m(\mathbf{v}_1 - \mathbf{v}_0)| \leq R$$

where

$$t_m = -\mathbf{v}_0.(\mathbf{v}_1 - \mathbf{v}_0)/|\mathbf{v}_1 - \mathbf{v}_0|^2$$

The points at which the edge cross the sphere are

$$|\mathbf{v}_1 - \mathbf{v}_0|^2 t^2 + 2\mathbf{v}_0.(\mathbf{v}_1 - \mathbf{v}_0)t + \mathbf{v}_0.\mathbf{v}_0 - R^2 = 0$$

If one of these roots lies in $[0, 1]$ an intersection point has been found. The point $\mathbf{v}_0 + t_m(\mathbf{v}_1 - \mathbf{v}_0)$ can be used to interpolate values from the centers of the intersecting balls (it lies on the simplex formed by the projected centers of the balls whose intersection

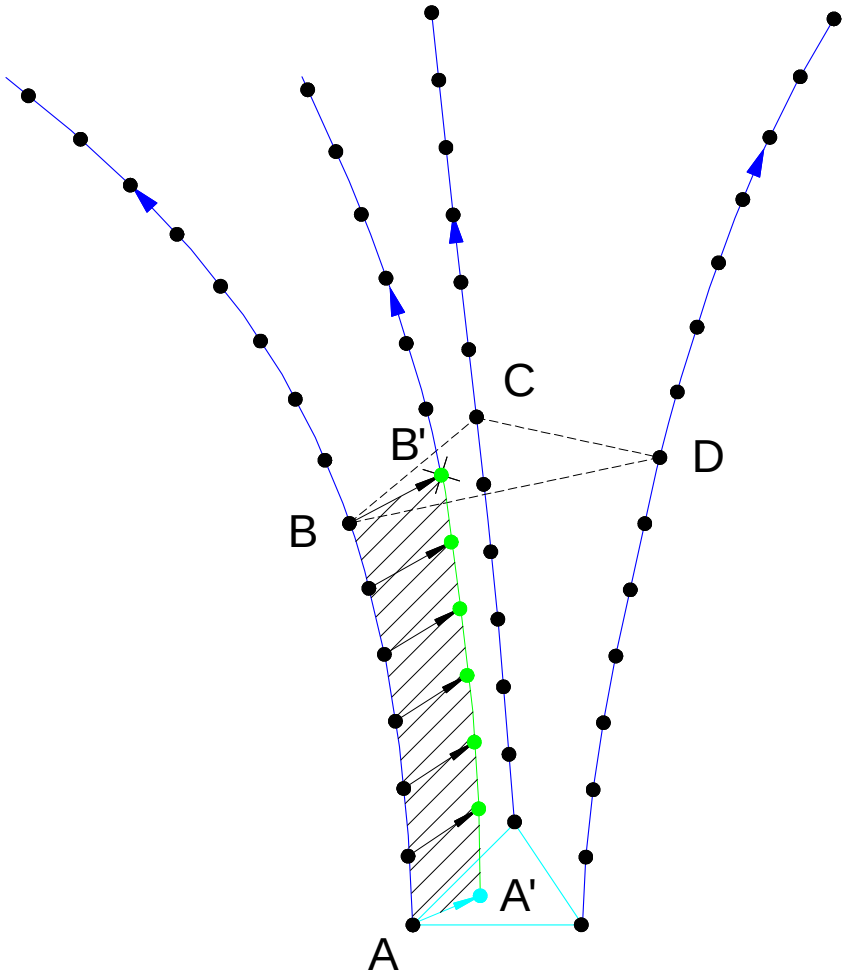

FIG. 4.4. *The interpolation algorithm. The point B', which lies on an edge of the polyhedron of the ball centered at B is found using the optimization problem. B' ay be interpolated from points B, C, and D (there are k corners in k-d), or found using a simple homotopy on the two point boundary value problem for a trajectory starting on $\mathbf{c}(\sigma)$ and ending on a line from B to B'.*

defines the edge). Note that in order to interpolate Taylor series expansions on a simplex they must be put into a common reference frame.

Another, more accurate approach is to interpolate the entire trajectory passing through the point on the dual simplex from the trajectories passing through the centers of the intersecting balls, and use that as an initial guess to a two point boundary

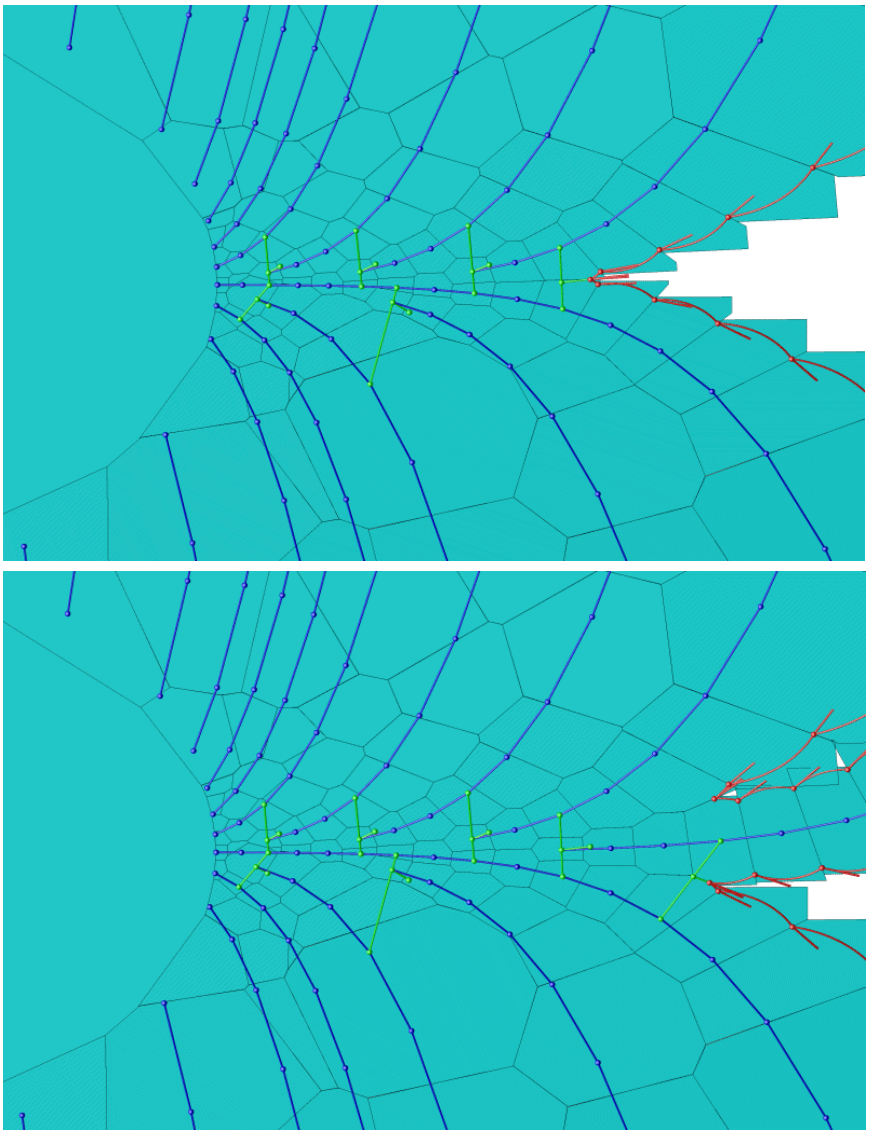

FIG. 4.5. *The behavior of the interpolation algorithm in the Lorenz system (the stable manifold of the origin near the origin). The blue points are the computed points on the manifold. The blue lines connect them along trajectories. The black polygons are the polyhedra associated with the points (the points do not necessarily lie in the polygon). The green edges are the dual simplices used to interpolate a new starting point, and the short green edges connect the minimizing points to the dual edges parallel to the flow. The red circles make up the boundary of U, and the red lines on the boundary are unit vectors parallel to the flow.*

value solver for the problem:

$$\mathbf{u}_{,\tau} = T\mathbf{F}/(F^p F^p)^{-1/2}$$

$$\mathbf{u}(0) = \mathbf{c}(\sigma)$$

$$\Phi_i^T(\mathbf{u}(1) - \mathbf{u}_i) = \mathbf{v}_0 + t_m(\mathbf{v}_1 - \mathbf{v}_0)$$

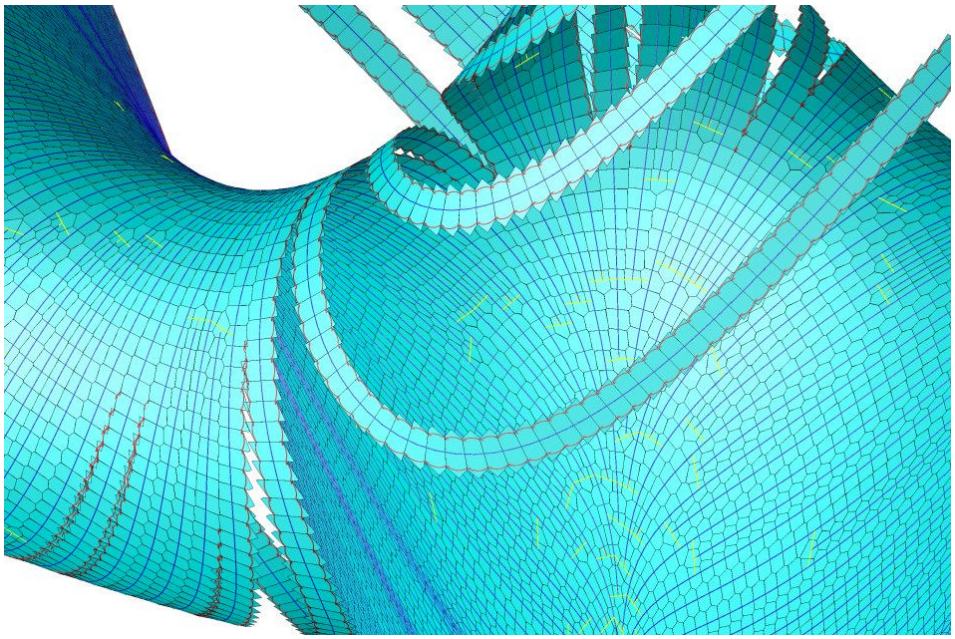

FIG. 4.6. *The behavior of the interpolation algorithm in the Lorenz system (the stable manifold of the origin far from the origin).*

where i is the ball on which the intersecting edge has been found. This generates a set of point covering the invariant manifold for which every point lies on a trajectory starting on the initial curve.

4.4. Measuring distances on the invariant manifold. This method does not give a global parameterization. This may cause difficulties when trying to determine if two balls overlap, since if the balls lie on different sheets, they may be near in $\mathbb{R}^n$, but not in the (t, σ) parameterization (Figure 4.7).

For implicitly defined manifolds (i.e. solutions of $F(u) = 0$) we know that if the Jacobian F_u is nonsingular at a point on the manifold, the manifold is locally unique. So it is possible to put a small box around a piece of the computed manifold and make a useful assertion about there being a unique piece of the manifold inside the box. By contrast, invariant manifolds are globlal in nature, and it is not hard to find examples where there is a countable infinity of sheets of the manifold in any such box, without any degeneracy in the flow. (A simple example is a trajectory in a 2-d phase plane which spirals onto a periodic motion. See Fig. 4.7.)

Points may be marked using the original parameterization (t, σ), and distance measured in that space. These can be tracked quite simply using

$$\begin{pmatrix} t \\ \sigma \end{pmatrix}' = \begin{pmatrix} 1 \\ 0 \end{pmatrix}$$

along a trajectory, and interpolating them along with $\mathbf{u}$.

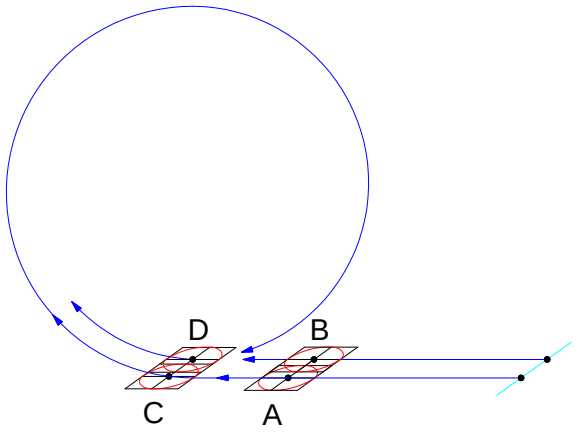

FIG. 4.7. *Determining whether two charts overlap. An invariant manifold is shown which spirals exponentially onto a cylinder. Chart C is close to A in both the phase space and the (t, σ) parameter space, but without knowing the (t, σ) parameters of D it is numerically impossible to tell if D is the image of B, or of C after a turn around the cylinder.*

5. The stable manifold of the origin in the Lorenz system. The Lorenz system [11], [30], is

$$\frac{\mathrm{d}}{\mathrm{d}t}u^0 = \sigma(u^1 - u^0)$$

$$\frac{\mathrm{d}}{\mathrm{d}t}u^1 = \rho u^0 - u^1 - u^0 u^2$$

$$\frac{\mathrm{d}}{\mathrm{d}t}u^2 = u^0 u^1 - \beta u^2$$

We will use the "standard" parameter values $\sigma = 10$, $\rho = 28$ and $\beta = 8/3$. In Appendix C we derive formulae for the coefficients in a third order expansion for an invariant manifold of a hyperbolic fixed point. This gives, for the stable manifold at the origin

$$u_{,0} = (-0.6148168, 0.7886700, 0),\ u_{,1} = (0, 0, 1)$$
$$v_0 = (0.7886700, 0.6148168, 0)$$

$$u(s,t) \sim s u_{,0} + t u_{,1}$$
$$+ s(6.114934 \cdot 10^{-5} s^2 - 1.012804 \cdot 10^{-2} t - 1.994442 \cdot 10^{-4} t^2) v_0$$

The z-axis is part of the stable manifold of the origin, and it is useful to examine a fat trajectory on the z-axis. On $x = y = 0$ we have

$$\mathbf{F} = (0, 0, -\beta u^2) \qquad \mathbf{F_u} = \begin{pmatrix} -\sigma & \sigma & 0 \\ \rho - u^2 & -1 & 0 \\ 0 & 0 & -\beta \end{pmatrix}$$

$$F^i_{,j,k} = 0, \text{ except } F^1_{,0,2} = -1, \qquad F^2_{,0,1} = 1$$

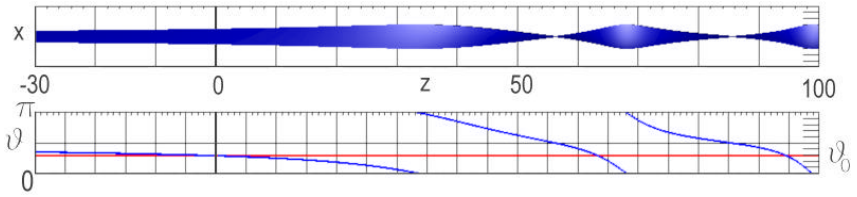

FIG. 5.1. *The $u^i_{,1}$ tangent of the stable manifold of the origin in the Lorenz system at the standard parameter values on the z-axis. The $\mathbf{u}_{,0}$ tangent is simply $(0,0,1)$, and $\mathbf{u}_{,1} = (\cos\theta, \sin\theta, 0)$. The tangents at $z = 0$ may be found from the stable eigenvectors, and we find that $\theta_0 = -0.90863$.*

With the ansatz that $u^i_{,0} = (0, 0, \pm 1)$ and $u^i_{,1} = (\cos\theta, \sin\theta, 0)$, the equations for the evolution of the two tangent vectors are

$$\begin{aligned}
\beta|z|u^i_{,\tau} &= (0, 0, \beta z) \qquad u^i = (0, 0, \pm\tau) \\
u^i_{,0} &= (0, 0, z/|z|) \qquad \beta|z|u^i_{,0,\tau} = (0, 0, 0) \\
u^i_{,1} &= (\cos\theta, \sin\theta, 0) \\
\beta|z|\theta_{,\tau} &= \sigma \sin^2\theta - (\rho - z)\cos^2\theta - (\sigma - 1)\cos\theta\sin\theta
\end{aligned}$$

We have

$$\rho\cos^2\theta_0 - \sigma\sin^2\theta_0 + (\sigma - 1)\cos\theta_0\sin\theta_0 = 0$$

so as $z \to 0$ the equation for $\theta_{,z}(0)$ approaches

$$\beta\theta_{,z}(0) = \mp\cos^2\theta(0)$$

And, at the "standard" parameters, we have $\theta_0 = -0.90863$.

Figures 5.2 and 5.3 show two computations of the unstable manifold of the origin for different time intervals. The cross sections ($x = 0$, $y = 0$ and $z = 27$) are suggestive of a structure that might be extrapolated to longer time.

6. Conclusions. This algorithm finds a uniform distribution of points on an invariant manifold by integrating local coordinate patches as points on fat trajectories. The error along the trajectory depends on the error in the initial condition, and the integration error. To begin, trajectories start at a point on the local expansion of the invariant manifold of the fixed point. So there are three sources of error: error in the initial evaluation of the expansion about the fixed point, error integrating a fat trajectory, and error in interpolation of a starting point for a new trajectory.

The error in the initial point on $\mathbf{c}(\lambda)$ can be controlled by the order of approximation and radius of the initial sphere. The error in the fat trajectory is determined by the integration scheme. The center of the fat trajectory may be integrated using the "best" available integration for the system – the equations are the same as the original system. The tangent and second derivatives evolve according to modified linearizations of the flow, but the effect of error in these terms devolves onto the interpolation.

We proposed two interpolation schemes. The first, used in the example, is Hermite interpolation on a simplex. The second interpolates a trajectory back to $\mathbf{c}(\sigma)$ on the same simplex, and uses a two point boundary value solver to refine this approximation. The second method is superior, and produces a surface for which every point lies on a trajectory back to the initial curve.

Any point u_f on the computed surface is near a piecewise trajectory which begins on the initial curve. The computed surface consists of neighborhoods of trajectories, and u_f lies in such a neighborhood, on a fat trajectory which began at a point on another fat trajectory. Thus the trajectories can be "walked" backward in time to a point on the initial curve. The path generated is not continuous, unless the second type of interpolation is used. However, this approximate trajectory may be used as an initial guess to a two point boundary value problem for a trajectory starting on the initial curve (n conditions, $k-1$ unknowns σ), and ending after time T at a point whose projection onto the tangent plane at u_f is u_f (k conditions, 1 additional unknown T). This is a set of n ODE's with initial conditions, and k parameters (T, σ) with k auxilliary algebraic constraints.

$$u^i_{,\tau} = TF^i/(F^pF^p)^{-1/2}$$

$$u^i(0) = c^i(\sigma)$$

$$u^p_{,j}(u^p(1) - u^p_f) = 0$$

This approach attempts to minimize the amount of interpolation that is done, and to allow higher order interpolation to be used. It avoids the recomputation that is done by Doedel's algorithm, using a local approximation in areas where trajectories needed to cover the manifold to a specified density lie close together.

Our results for the Lorenz manifold are qualitatively the same as the computations of [24], [23] and [12], and to the sketches in [1]. Note that contours of our scaled time τ are not the same as Krauskopf and Osinga's geodesic rings. We measure distance along trajectories, and they use an approximate geodesic distance on the manifold.

The main advantage of this method appears to be the ability to compute the entire manifold for quite long distances in time. Doedel has recently computed parts of the manifold for equally long times, but misses a neighborhood of the z-axis.

Appendix A. The image of a surface under the flow.

Below we derive the evolution equations of a fat trajectory. A fat trajectory is a trajectory with a locally orthonormal coordinate system at each point on the trajectory, together with a second order approximation to the invariant manifold.

A.1. The global parameterization. The image under the flow of a $(k-1)$ dimensional surface $c^i(\sigma)$ that is transverse to the flow,

$$F^i(\mathbf{c}) \notin \text{span}(\{c^i_{,\sigma_j}\})$$

is a k dimensional surface. It can be globally parameterized by σ and t –

$$u^i(t,\sigma) \equiv c^i(\sigma) + \int_0^t F^i(u(\tau,\sigma))\ d\tau \tag{A.1}$$

From this expression we obtain the basis for the tangent space

$$u^i_{,t} = F^i \qquad u^i_{,\sigma_j}(t,\sigma) = c^i_{,\sigma_j}(\sigma) + \int_0^t F^i_{,p} u^p_{,\sigma_j}(\tau,\sigma)\ d\tau \tag{A.2}$$

If $\mathbf{c}(\sigma)$ is well parameterized (i.e. the vectors $\mathbf{c}_{,\sigma_j}$ are linearly independant), and if the flow is transverse to $c(\sigma)$ then at $t = 0$ the vectors $u^i_{,t}$ and $u^i_{,\sigma_j}$ span the k-dimensional tangent space of the invariant manifold. An evolution equation can be

written for $u^i_{,\sigma_j}(t,\sigma)$:

$$u^i_{,t,\sigma_j} = F^i_{,p} u^p_{,\sigma_j} \qquad\qquad u^i_{,\sigma_j}(\sigma,0) = c^i_{,\sigma_j}(\sigma)$$

Differentiating (Eqs. A.2) again, we have

$$\begin{aligned} u^i_{,t,t} &= F^i_{,p} u^p_{,t} \\ u^i_{,t,\sigma_j} &= F^i_{,p} u^p_{,\sigma_j} \\ u^i_{,\sigma_j,\sigma_k} &= c^i_{,\sigma_j,\sigma_k} + \int_0^t \left(F^i_{,p} u^p_{,\sigma_j,\sigma_k} + F^i_{,p,q} u^p_{,\sigma_j} u^q_{,\sigma_k} \right) d\tau \end{aligned} \tag{A.3}$$

With the corresponding evolution equation for $u^i_{,\sigma_j,\sigma_k}$ being

$$u^i_{,t,\sigma_j,\sigma_k} = F^i_{,p} u^p_{,\sigma_j,\sigma_k} + F^i_{,p,q} u^p_{,\sigma_j} u^q_{,\sigma_k} \qquad\qquad u^i_{,\sigma_j,\sigma_k}(\sigma,0) = c^i_{,\sigma_j,\sigma_k}(\sigma)$$

These ($u^i_{,t}$, $u^i_{,t,\sigma_j}$, and $u^i_{,t,\sigma_j,\sigma_k}$) are enough for us to solve an initial value problem for a second order expansion of the invariant manifold near a trajectory. We will call this a "fat trajectory", since in some sense it is a narrow strip of the invariant manifold near the trajectory.

As was discussed in the introduction, this parameterization has some undesirable properties. So we propose to reparameterize the surface near a trajectory based on arclength, by deriving expressions for the evolution of a Euclidean basis for the invariant manifold and its derivatives along a trajectory.

A.2. A coordinate that corresponds to arclength along a trajectory. We first reparameterize the trajectory, introducing an arclength parameter τ.

$$t = T(\tau) \qquad \longrightarrow \qquad u^i_{,\tau} = T_{,\tau} u^i_{,t}$$

Then we require that

$$T_{,\tau} T_{,\tau} u^i_{,t} u^i_{,t} = 1$$

so

$$T_{,\tau} = (F^p F^p)^{-1/2}, \qquad \text{and} \qquad u^i_{,\tau} = (F^p F^p)^{-1/2} F^i.$$

While this is reasonable geometrically, it assumes that the flow on the invariant manifold is not zero. Obviously the invariant manifolds associated with fixed points violate this condition, and it sometimes happens that a second fixed point lies on the manifold (as happens in the Lorenz example). It may also occur for invariant manifolds associated with a periodic orbit. Johnson, Jolly and Kevrekidis [20] suggest working in $\mathbb{R}^n \times \mathbb{R}$ where the time t is used as a last coordinate. This gives instead

$$T_{,\tau} = (F^p F^p + 1)^{-1/2}, \qquad \text{and} \qquad u^i_{,\tau} = (F^p F^p + 1)^{-1/2} F^i.$$

This eliminates the problem of "stagnation" points on the invariant manifold. I'm not sure what the advantage is, but if this inner product is used, it should probably be used throughout. Note that this is similar to "lifting" to convert non-autonomous systems to autonomous systems by adding an additional variable τ and equation $\tau_{,t} = 1$.

A.3. The evolution of a locally Euclidean coordinate system along a trajectory. We now wish to find a coordinate transformation for which the new coordinates are locally orthonormal. With $\xi^0 = \tau$, and $\xi^i = \sigma_i$, the transform is

$$\xi^i = X^i(s^0, ..., s^{k-1})$$

The chain rule applied to the coordinate transformation gives us the relation between the derivatives of the manifold in the two coordinate systems:

$$u^i_{,j} = X^p_{,j} u^i_{,\xi^p}$$

$$u^i_{,j,k} = X^p_{,j} X^q_{,k} u^i_{,\xi^p,\xi^q} + X^p_{,j,k} u^i_{,\xi^p}$$

$$u^i_{,j,k,l} = X^p_{,k} X^q_{,l} X^r_{,j} u^i_{,\xi^p,\xi^q,\xi^r} + \left(X^p_{,j,k} X^q_{,l} + X^p_{,j} X^q_{,k,l} + X^p_{,k} X^q_{,j,l} \right) u^i_{,\xi^p,\xi^q} + X^p_{,j,k,l} u^i_{,\xi^p}$$

We want to choose the transformation so that the new coordinates are orthonormal. The derivation is easier if we first derive expressions relating the metric and connection in the two systems, and then use those to determine the transformation.

Substituting into the definitions of the metric, connection and third forms, we find that

$$g_{ij} = X^p_{,i} X^q_{,j} g_{\xi^p \xi^q}$$

$$\Gamma_{ijk} = X^p_{,i} X^q_{,j} X^r_{,k} \Gamma_{\xi^p \xi^q \xi^r} + X^p_{,i} X^q_{,j,k} g_{\xi^p \xi^q}$$

$$\Gamma_{ijkl} = X^p_{,k} X^q_{,l} X^r_{,j} X^w_{,i} \Gamma_{\xi^w \xi^p \xi^q \xi^r} + \left(X^p_{,j,k} X^q_{,l} + X^p_{,j} X^q_{,k,l} + X^p_{,k} X^q_{,j,l} \right) X^w_{,i} \Gamma_{\xi^w \xi^p \xi^q} + X^p_{,j,k,l} X^q_{,i} g_{\xi^p \xi^q}$$

Let Y^i_j be the inverse of $X^i_{,j}$ –

$$Y^p_i X^j_{,p} = \delta^j_i \qquad\qquad Y^i_p X^p_{,j} = \delta^i_j$$

we then have

$$Y^p_j g_{ip} = X^p_{,i} g_{\xi^p \xi^j}$$

and

$$u^i_{,\xi^q} = Y^p_q u^i_{,p} \qquad\qquad u^i_{,\xi^p,\xi^q} = Y^v_q Y^r_p u^i_{,r,v} - Y^v_q Y^r_p X^w_{,r,v} u^i_{,\xi^w}$$

To integrate along the trajectory we need the derivatives

$$u^i_{,\xi^0,j} = X^r_{,j} u^i_{,\xi^0,\xi^r} + Y^p_0 X^q_{,p,j} u^i_{,\xi^q}$$

$$u^i_{,\xi^0,j,k} = X^p_{,j} X^q_{,k} u^i_{,\xi^0,\xi^p,\xi^q} + X^q_{,j,k} u^i_{,\xi^0,\xi^q} + Y^p_0 \left(X^w_{,p,j} X^q_{,k} + X^w_{,j} X^q_{,p,k} \right) u^i_{,\xi^w,\xi^q} + Y^p_0 X^w_{,p,j,k} u^i_{,\xi^w}$$

Straight substitution for the unknown quantities $u^i_{,\xi^p}$ and $u^i_{,\xi^p,\xi^q}$ gives

$$
\begin{aligned}
u^i_{,\xi^0,j} &= X^r_{,j} u^i_{,\xi^0,\xi^r} + Y^p_0 X^q_{,p,j} Y^r_q u^i_{,r} \\
u^i_{,\xi^0,j,k} &= X^p_{,j} X^q_{,k} u^i_{,\xi^0,\xi^p,\xi^q} + X^q_{,j,k} u^i_{,\xi^0,\xi^q} \\
&\quad + Y^p_0 \left(X^w_{,p,j} X^q_{,k} + X^w_{,j} X^q_{,p,k} \right) Y^v_q Y^r_w u^i_{,r,v} \\
&\quad + Y^p_0 \left(X^w_{,p,j,k} - \left(X^z_{,p,j} X^q_{,k} + X^z_{,j} X^q_{,p,k} \right) Y^v_q Y^r_z X^w_{,r,v} \right) Y^a_w u^i_{,a}
\end{aligned}
\tag{A.4}
$$

The metric and connection in the new coordinate system determine the higher derivatives of the transform, so we should be able to replace those derivatives with expressions involving the metric and connection. (The first order terms are not completely determined by the metric, as there are many orthonormal coordinate systems). If we operate on the equations for Γ_{ijk} and Γ_{ijkl} with $Y^j_0 g^{iw}$ (g^{ij} is the inverse of g_{ij}), and rearrange we obtain the expressions

$$
\begin{aligned}
Y^j_0 X^q_{,j,k} Y^w_q &= Y^j_0 g^{iw} \Gamma_{ijk} - g^{iw} X^p_{,i} X^r_{,k} \Gamma_{\xi^p \xi^0 \xi^r} \\
Y^p_0 \left(X^a_{,p,j,k} - \left(X^z_{,p,j} X^q_{,k} + X^z_{,j} X^q_{,p,k} \right) Y^v_q Y^r_z X^a_{,r,v} \right) Y^w_a &= \\
& Y^p_0 g^{iw} \Gamma_{ipjk} - g^{iw} X^p_{,j} X^q_{,k} X^a_{,i} \Gamma_{\xi^a \xi^0 \xi^p \xi^q} - g^{iw} X^q_{,j,k} X^a_{,i} \Gamma_{\xi^a \xi^0 \xi^q} \\
& - g^{iw} Y^p_0 \left(X^a_{,p,j} X^q_{,k} + X^a_{,j} X^q_{,p,k} \right) Y^b_q Y^r_a \Gamma_{irb}
\end{aligned}
$$

These are the same as the terms in Eq. (A.4). Substituting, we have that

$$
\begin{aligned}
u^i_{,\xi^0,j} &= X^r_{,j} u^i_{,\xi^0,\xi^r} + Y^p_0 g^{ra} \Gamma_{apj} u^i_{,r} - g^{ra} X^p_{,a} X^q_{,j} \Gamma_{\xi^p \xi^0 \xi^q} u^i_{,r} \\
u^i_{,\xi^0,j,k} &= X^p_{,j} X^q_{,k} u^i_{,\xi^0,\xi^p,\xi^q} + X^q_{,j,k} u^i_{,\xi^0,\xi^q} \\
&\quad + Y^p_0 \left(g^{br} \Gamma_{bpj} \delta^v_k + g^{bv} \Gamma_{bpk} \delta^r_j \right) \left(u^i_{,r,v} - g^{ba} \Gamma_{brv} u^i_{,a} \right) \\
&\quad - \left(X^p_{,a} X^q_{,j} g^{ar} \delta^v_k + X^p_{,a} X^q_{,k} g^{av} \delta^r_j \right) \left(u^i_{,r,v} - g^{aw} \Gamma_{arv} u^i_{,w} \right) \Gamma_{\xi^p \xi^0 \xi^q} \\
&\quad + \left(Y^p_0 \Gamma_{apjk} - X^p_{,j} X^q_{,k} X^w_{,a} \Gamma_{\xi^w \xi^0 \xi^p \xi^q} - X^q_{,j,k} X^w_{,a} \Gamma_{\xi^w \xi^0 \xi^q} \right) g^{ar} u^i_{,r}
\end{aligned}
$$

We have left some of the second order terms that with hindsight we know will be needed. These equations hold for any such transformation, though in general they are probably not of much interest.

A.4. The metric and connection for the invariant manifold.

A.4.1. In the coordinates $(\tau, \sigma_{,j})$. The original parametization of the invariant manifold, given by the integral equation (A.1) has a particular metric $g_{\xi^i \xi^j}$ and connection $\Gamma_{\xi^i \xi^j \xi^k}$. The derivatives that we know explicitly (i.e. without integrals)

are

$$
\begin{aligned}
u^i_{,\xi^0} &= T_{,\tau} F^i \\
u^i_{,\xi^0,\xi^j} &= T_{,\tau} F^i_{,p} u^p_{,\xi^j} \\
u^i_{,\xi^0,\xi^j,\xi^k} &= T_{,\tau} \left(F^i_{,p} u^p_{,\xi^j,\xi^k} + F^i_{,p,q} u^p_{,\xi^j} u^q_{,\xi^k} \right)
\end{aligned}
$$

so

$$
\begin{aligned}
g_{\xi^0\xi^0} &= T^2_{,\tau} F^p F^p = 1 \\
\Gamma_{\xi^i\xi^0\xi^j} &= T_{,\tau} u^q_{,\xi^i} F^q_{,p} u^p_{,\xi^j} \\
\Gamma_{\xi^i\xi^0\xi^j\xi^k} &= T_{,\tau} \left(u^q_{,\xi^i} F^q_{,p} u^p_{,\xi^j,\xi^k} + u^r_{,\xi^i} F^r_{,p,q} u^p_{,\xi^j} u^q_{,\xi^k} \right).
\end{aligned}
$$

Recall that $T_{,\tau} = (F^p F^p)^{-1/2}$.

A.4.2. In the new coordinates s^j. There are several possibilities for choosing the metric, connection and third forms in the new coordinate system. The connection and third forms are constrained by

$$(g_{ij})_{,k} = \Gamma_{ijk} + \Gamma_{jik}$$

$$(\Gamma_{ijk})_{,l} = \Gamma_{ijkl} + u^w_{,i,l} u^w_{,j,k}$$

but beyond that we are free to choose whatever connection and third forms are convenient.

A.4.3. Riemannian normal coordinates. One coordinate system, which is popular in the theory of Gravitation is Riemannian normal coordinates (RNC). These are defined by $g_{ij} = \delta_{ij}$ and $\Gamma_{ijk} = 0$, which certainly satsify $\Gamma_{ijk} + \Gamma_{jik} = (g_{ij})_{,k} = 0$. The constraint on the third form is

$$\Gamma_{ijkl} = -u^w_{,i,l} u^w_{,j,k}$$

RNC are a coordinate system that changes as little as possible from frame to frame. In RNC Eqs. (A.4) become

$$
\begin{aligned}
u^i_{,\xi^0,j} &= X^r_{,j} u^i_{,\xi^0,\xi^r} - \delta^{ra} X^p_{,a} X^q_{,j} \Gamma_{\xi^p\xi^0\xi^q} u^i_{,r} \\
u^i_{,\xi^0,j,k} &= X^p_{,j} X^q_{,k} u^i_{,\xi^0,\xi^p,\xi^q} + X^q_{,j,k} u^i_{,\xi^0,\xi^q} - X^p_{,a} \left(X^q_{,j} u^i_{,r,k} \delta^{ar} + X^q_{,k} u^i_{,j,v} \delta^{av} \right) \Gamma_{\xi^p\xi^0\xi^q} \\
&\quad + \left(Y^p_0 \Gamma_{apjk} - X^p_{,j} X^q_{,k} X^w_{,a} \Gamma_{\xi^w\xi^0\xi^p\xi^q} - X^q_{,j,k} X^w_{,a} \Gamma_{\xi^w\xi^0\xi^q} \right) \delta^{ar} u^i_{,r}
\end{aligned}
$$

which is still independant of the surface, merely a choice of the new coordinate system.

A.4.4. Riemannian normal coordinates on the invariant manifold. Now we substitute the connection and third form in the old coordinates.

$$T_{,\tau}^{-1}u^i_{,\xi^0,j} = F^i_p\left(X^r_{,j}u^p_{,\xi^r}\right) - \left(X^p_{,r}u^v_{,\xi^p}\right)F^v_{,w}\left(X^q_{,j}u^w_{,\xi^q}\right)u^i_{,r}$$

$$\begin{aligned}T_{,\tau}^{-1}u^i_{,\xi^0,j,k} &= F^i_{,r}\left(X^p_{,j}X^q_{,k}u^r_{,\xi^p,\xi^q} + X^p_{,j,k}u^r_{,\xi^p}\right) + F^i_{,r,w}\left(X^p_{,j}u^r_{,\xi^p}\right)\left(X^q_{,k}u^w_{,\xi^q}\right)\\ &- \left(X^p_{,r}u^v_{,\xi^p}\right)F^v_{,w}\left(X^a_{,j}u^w_{,\xi^a}\right)u^i_{,r,k} - \left(X^b_{,v}u^v_{,\xi^b}\right)F^v_{,w}\left(X^a_{,k}u^w_{,\xi^a}\right)u^i_{,j,v}\\ &- \left(X^w_{,a}u^b_{,\xi^w}\right)F^b_{,z}\left(X^p_{,j}X^q_{,k}u^z_{,\xi^p,\xi^q} + X^q_{,j,k}u^z_{,\xi^q}\right)u^i_{,a}\\ &- \left(X^w_{,a}u^r_{,\xi^w}\right)F^r_{,z,b}\left(X^p_{,j}u^z_{,\xi^p}\right)\left(X^q_{,k}u^b_{,\xi^q}\right)u^i_{,a} - Y^p_0u^w_{,a,p}u^w_{,j,k}u^i_{,a}\end{aligned}$$

And finally, we use the chain rule to replace derivatives wrt. the old coordinates with derivatives wrt. the new coordinates (this is why we left those second derivatives of the transform)

$$T_{,\tau}^{-1}u^i_{,\xi^0,j} = F^i_pu^p_{,j} - u^p_{,r}F^p_{,q}u^q_{,j}u^i_{,r}$$

$$\begin{aligned}T_{,\tau}^{-1}u^i_{,\xi^0,j,k} &= F^i_{,p}u^p_{,j,k} + F^i_{,p,q}u^p_{,j}u^q_{,k} - u^p_{,r}F^p_{,q}u^q_{,j}u^i_{,r,k} - u^p_{,r}F^p_{,q}u^q_{,k}u^i_{,j,r}\\ &- \left(u^p_{,w}F^p_{,q}u^q_{,j,k} + u^p_{,w}F^p_{,q,r}u^q_{,j}u^r_{,k} + Y^p_0u^q_{,w,p}u^q_{,j,k}\right)u^i_{,w}\end{aligned}$$

The only troublesome term is $Y^p_0u^q_{,w,k}u^q_{,p,j}u^i_{,w}$. Again using the chain rule, we have

$$Y^p_0u^q_{,p,w} = u^q_{,\xi^0,w} = F^q_pu^p_{,w} - u^p_{,r}F^p_{,v}u^v_{,w}u^q_{,r}$$

so

$$Y^p_0u^q_{,p,w}u^q_{,j,k} = u^q_{,j,k}F^q_pu^p_{,w} - u^p_{,r}F^p_{,v}u^v_{,w}u^q_{,r}u^q_{,j,k}$$

and, since $u^q_{,r}u^q_{,j,k} = \Gamma_{rjk} = 0$,

$$\begin{aligned}T_{,\tau}^{-1}u^i_{,\xi^0,j,k} &= F^i_{,p}u^p_{,j,k} + F^i_{,p,q}u^p_{,j}u^q_{,k} - u^p_{,r}F^p_{,q}u^q_{,j}u^i_{,r,k} - u^p_{,r}F^p_{,q}u^q_{,k}u^i_{,j,r}\\ &- \left(u^p_{,w}F^p_{,q}u^q_{,j,k} + u^p_{,w}F^p_{,q,r}u^q_{,j}u^r_{,k} + u^p_{,j,k}F^p_qu^q_{,w}\right)u^i_{,w}\end{aligned}$$

So we have dervived a set of evolution equations for the second order expansion of the invariant manifold in RNC.

A.5. Summary. In Riemannian normal coordinates the evolution equations of a second order approximation to the invariant manifold are

$$u^i_{,\tau} = (F^wF^w)^{-1/2}F^i$$

$$u^i_{,\tau,j} = (F^wF^w)^{-1/2}\left(F^i_{,p}u^p_{,j} - u^p_{,r}F^p_{,q}u^q_{,j}u^i_{,r}\right)$$

$$\begin{aligned}u^i_{,\tau,j,k} &= (F^wF^w)^{-1/2}\left(F^i_{,p}u^p_{,j,k} + F^i_{,p,q}u^p_{,j}u^q_{,k} - u^p_{,r}F^p_{,q}u^q_{,j}u^i_{,r,k} - u^p_{,r}F^p_{,q}u^q_{,k}u^i_{,j,r}\right)\\ &-(F^wF^w)^{-1/2}\left(u^p_{,r}F^p_{,q}u^q_{,j,k} + u^p_{,r}F^p_{,q,v}u^q_{,j}u^v_{,k} + u^p_{,j,k}F^p_qu^q_{,r}\right)u^i_{,r}\end{aligned}$$

These allow us to integrate in the τ direction (scaled time), to find u^i, $u^i_{,j}$, and $u^i_{,j,k}$ at points along the trajectory. Remember that repeated indices (p, q, r, w and v) stand for summations over those indices and that a comma in front of an index stands for the partial derivative wrt that index. The second order approximation at τ is

$$u^i(s) \sim u^i + u^i_j s^j + \frac{1}{2} u^i_{,j,k} s^j s^k$$

A.6. Initial conditions. Given a point u^i and first and second derivatives of the surface $c^i_{,\sigma_j}$ and $c^i_{,\sigma_j,\sigma_k}$, we find an initial basis $u^i_{,j}$ and second derivatives $u^i_{,j,k}$. This is done by finding initial transformation derivatives $X^i_{,j}$ and $X^i_{,j,k}$. With

$$\begin{array}{lll} g_{\xi^0,\xi^0} = F^p F^p & \Gamma_{\xi^0\xi^0,\xi^0} = F^p F^p_{,q} F^q & \Gamma_{\xi^i\xi^0,\xi^0} = c^p_{,\sigma_i} F^p_{,q} F^q \\ g_{\xi^0,\xi^i} = F^p c^p_{,\sigma_i} & \Gamma_{\xi^0\xi^0,\xi^i} = F^p F^p_{,q} c^q_{,\sigma_i} & \Gamma_{\xi^i\xi^0,\xi^j} = c^p_{,\sigma_i} F^p_{,q} c^q_{,\sigma_j} \\ g_{\xi^i,\xi^j} = c^p_{,\sigma_i} c^p_{,\sigma_j} & \Gamma_{\xi^0\xi^i,\xi^j} = F^p c^p_{,\sigma_j,\sigma_k} & \Gamma_{\xi^i\xi^j,\xi^k} = c^p_{,\sigma_i} c^p_{,\sigma_j,\sigma_k} \end{array}$$

We first find an orthonormal basis $u^i_{,j}$ from $\{F^i, c^i_{,\sigma_j}\}$ by the Gram–Schmidt orthogonalization procedure, then solve the linear systems (one for each j, with a different right hand side for each k)

$$g_{\xi^i,\xi^j} X^i_{,k} = u^p_{,k} u^p_{,\xi^j}$$

for $X^i_{,j}$. If the flow is transverse to the initial curve c, the metric $g_{\xi^i\xi^j}$ is non-singular. The second derivatives are then explicitly given by

$$X^i_{,j,k} = X^i_{,z} \Gamma_{zjk} - X^i_{,z} X^p_{,z} X^q_{,j} X^r_{,k} \Gamma_{\xi^p\xi^q,\xi^r}$$

And then finally, the initial second derivatives in the new basis are given by

$$u^i_{,j,k} = X^p_{,j} X^q_{,k} u^i_{,\xi^p,\xi^q} + X^p_{,j,k} u^i_{,\xi^p}$$

Appendix B. Moving back toward $\mathbf{c}(\sigma)$ exterior to a union of balls on an invariant manifold.

In this appendix we derive the result used in Section 4.3 stating that if the balls are small relative to the curvature of $M_{\mathbf{c}}$, and the flow $\mathbf{F}$ ($\mathbf{F}$ is nearly constant over a ball), an interpolation point of a certain form exists.

We formulate a problem similar to a constrained nonlinear optimization problem on the part of the manifold not yet covered, whose solution is a point as far back under the flow toward $\mathbf{c}(\sigma)$ as possible. We show that such a point exists, and use the KKT conditions [4] to characterize it.

Nonlinear optimization deals with gradient flows (the gradient of the objective), and $\mathbf{F}$ is in general not such a flow (in flat space with $k \leq 3$ gradient flows must satisfy $\nabla \times \mathbf{F} = 0$), so some care is needed. For example, the KKT conditions say that a mimimizer is an unstable stationary point (source) of the flow. This (obviously) holds for non-gradient flows as well, but other results, such as the existance of a minimizer, may not carry over.

We begin with a finite piece of the manifold of starting points $\mathbf{c}(\Omega_\sigma)$, and the invariant manifold associated with it:

$$\mathcal{M} = \mathbf{u}([-T, T], \Omega_\sigma),$$

where, again

$$\mathbf{u}(t,\sigma) = \mathbf{c}(\sigma) + \int_0^t \mathbf{F}(\mathbf{u}(\tau,\sigma))\mathrm{d}\tau.$$

In addition, we have a set of N points $\mathbf{u}_i = \mathbf{u}(t_i,\sigma_i) \in \mathcal{M}$, each with a tangent space spanned by the columns of an orthonormal matrix Φ_i, and a radius R_i. We are going to assume that $\mathbf{c}(\Omega_\sigma)$ is covered by the balls (if not, fat trajectories can be chosen to do so), and that Ω_σ has a boundary whose image under the flow $\mathbf{u}([-T,T],\delta\Omega_\sigma)$ (the image of the boundary) is covered. If Ω_σ has no boundary, as is the case with the stable and unstable manifolds of a fixed point, an artificial boundary must be introduced. We have not said much about computing manifolds of pieces of $\mathbf{c}(\sigma)$, and only point out that the boundary of the boundary, $\mathbf{c}(\delta\Omega)$, has no boundary, and so we might first cover it using k dimensional fat trajectories, but interpolate as if it were a $k-1$ dimensional manifold. Applying this recursively reduces to the two dimensional case. For a two dimensional manifold this means integrating one fat trajectory before interpolating – hardly a strong assumption.

Each ball defines a neighborhood of $M_{\mathbf{c}(\Omega_\sigma)}$ about it's center –

$$\mathcal{N}_i = \left\{\mathbf{u} \in M_{\mathbf{c}(\Omega_\sigma)} \mid |\Phi_i^T(\mathbf{u}-\mathbf{u}_i)| \le R_i\right\}$$

(in addition, we require that points $\mathbf{u} \in \mathcal{N}_i$ lie near $\mathbf{u}_i$ in the (t,σ) parameterization, as points far away in $\mathbb{R}^n$ can project close to $\mathbf{u}_i$).

The feasible region U for the "optimization" problem is the complement of the union of the neighborhoods. If V is the interior of the union of the neighborhoods:

$$V = \bigcup_1^N \mathcal{N}_i$$

then

$$U = (\mathcal{M} - V) \bigcup \delta V$$

In U we define the flow

$$\tilde{\mathbf{F}} = -\mathbf{F} \qquad \text{for} \qquad \mathbf{u} \in \mathbf{u}((0,T],\Omega_\sigma) \bigcap U$$

$$\tilde{\mathbf{F}} = \quad \mathbf{F} \qquad \text{for} \qquad \mathbf{u} \in \mathbf{u}([-T,0),\Omega_\sigma) \bigcap U$$

If the flow is out of U anywhere along $\delta V \bigcap \mathcal{M}$, we use the flow induced on δV to prevent trajectories from leaving U.

If $\mathbf{u} \in \delta V \bigcap \mathbf{u}((0,T],\Omega_\sigma)$, and $\mathbf{F}(\mathbf{u}).\mathbf{n}(\mathbf{u}) < 0$, $\qquad \tilde{\mathbf{F}} = \mathbf{F} + (\mathbf{F}.\mathbf{n})\mathbf{n}$.

If $\mathbf{u} \in \delta V \bigcap \mathbf{u}([-T,0],\Omega_\sigma)$, and $-\mathbf{F}(\mathbf{u}).\mathbf{n}(\mathbf{u}) < 0$, $\qquad \tilde{\mathbf{F}} = -\mathbf{F} - (\mathbf{F}.\mathbf{n})\mathbf{n}$.

Since $\mathbf{c}(\Omega_\sigma) \bigcap U = \emptyset$, and $\mathbf{u}([-T,T],\delta\Omega_\sigma) \bigcap U = \emptyset$, the boundary of U is

$$\delta U = \left(\mathbf{u}(-T,\Omega_\sigma) \bigcap U\right) \bigcup \left(\mathbf{u}(T,\Omega_\sigma) \bigcap U\right) \bigcup \left(\delta V \bigcap \mathcal{M}\right).$$

Each trajectory of $\tilde{\mathbf{F}}$ which starts on $\mathbf{u}(-T,\Omega_\sigma) \bigcap U$ or $\mathbf{u}(T,\Omega_\sigma) \bigcap U$ enters U, and each trajectory of $\mathbf{F}$ which passes through a point in U also contains a point on

$\mathbf{c}(\Omega_\sigma) \subset V$. Therefore the image of U under $\tilde{\mathbf{F}}$ must approach one or more stable stationary points on $\delta V \bigcap \mathcal{M}$, and at least one such stationary point must exist. In fact there must be at least one stable stationary point in each of $\delta V \bigcap \mathcal{M} \bigcap \mathbf{u}([-T, 0), \Omega_\sigma)$ and $\delta V \bigcap \mathcal{M} \bigcap \mathbf{u}((0, T], \Omega_\sigma)$.

Points on δV lie on the boundary of one or more balls, and can be classified by that set of balls. Consider a point $\mathbf{u}_* \in \delta V \bigcap \mathcal{M}$ which lies on the intersection of the images of the $m \geq 1$ balls at the points $\left\{\mathbf{u}_{i_j}\right\}$ –

$$b_{i_j}(\mathbf{u}_*) = (\mathbf{u}_* - \mathbf{u}_{i_j})^T \Phi_{i_j} \Phi_{i_j}^T (\mathbf{u}_* - \mathbf{u}_{i_j}) - R_{i_j}^2 = 0, \qquad 0 \leq j < m$$

$$b_i(\mathbf{u}_*) = (\mathbf{u}_* - \mathbf{u}_{i_j})^T \Phi_i \Phi_i^T (\mathbf{u}_* - \mathbf{u}_{i_j}) - R_{i_j}^2 > 0, \qquad i \neq i_j,\ 0 \leq j < m$$

$$\mathbf{u}_* \in \mathcal{M}$$

The first order optimality (KKT) conditions [4] require that $\mathbf{u}_*$ be a stationary point of $\tilde{\mathbf{F}}$ –

$$\tilde{\mathbf{F}}(\mathbf{u}_*) = \sum_0^{j<m} \lambda_j \nabla b_{i_j}(\mathbf{u}_*) = 2 \sum_0^{j<m} \lambda_j \Phi_{i_j} \Phi_{i_j}^T (\mathbf{u}_* - \mathbf{u}_{i_j}) + \sum_0^{n-k} \mu_j \mathbf{n}_j$$

$$\lambda_j \geq 0$$

Here the vectors $\mathbf{n}_j$ are a basis for the normal space of $\mathcal{M}$ at $\mathbf{u}_*$. Since $\mathcal{M}$ is an invariant manifold under $\tilde{\mathbf{F}}$, $\tilde{\mathbf{F}}$ is in the tangent space of $\mathcal{M}$. We project this stationarity condition into that tangent space

$$\tilde{\mathbf{F}}(\mathbf{u}_*) = 2 \sum_0^{j<m} \lambda_j \Phi_* \Phi_*^T \Phi_{i_j} \Phi_{i_j}^T (\mathbf{u}_* - \mathbf{u}_{i_j}).$$

This is equivalent to

$$\Phi_{i_0}^T \left((\sum \tfrac{\lambda_j}{\lambda_T} \Phi_* \Phi_*^T \Phi_{i_j} \Phi_{i_j}^T) \mathbf{u}_* - \mathbf{u}_{i_0} \right) - \tfrac{1}{2\lambda_T} \Phi_{i_0}^T \mathbf{F}(\mathbf{u}_*) = \sum_0^{j<m} \tfrac{\lambda_j}{\lambda_T} \Phi_{i_0}^T \left(\Phi_* \Phi_*^T \Phi_{i_j} \Phi_{i_j}^T \mathbf{u}_{i_j} - \mathbf{u}_{i_0} \right)$$

where

$$\lambda_T = \sum \lambda_j$$

(We could project into the tangent space of any of the balls defining $\mathbf{u}_*$.)

Finding the intersection of the projection of m spheres is difficult, and we use the same approximation used in [15]. If the distance between the tangent spaces and the manifold is small within each ball, the tangent spaces are almost the same, and $\mathbf{u}_*$ is approximatly the intersection of the balls centered at the projections of the $\mathbf{u}_{i_j}$ with the same radii (R_{i_j}). There is an error committed here (which can be quantified using a Taylor series approximation to the manifold and tangent spaces) which is the same order of magnitude as the largest distance from the tangent space to the manifold.

This replaces the problem on $\mathcal{M}$ with a problem over the part of the polyhedron in each tangent space that lies inside the ball:

$$\mathbf{s}_* - \alpha \Phi_{i_0}^T \mathbf{F}(\mathbf{u}_*) = \sum_0^{j<m} \theta_j \Phi_{i_0}^T \left(\mathbf{u}_{i_j} - \mathbf{u}_{i_0} \right)$$

where

$$\alpha = \frac{1}{2\lambda_T}, \qquad \theta_j = \lambda_j/\lambda_T \geq 0, \qquad \sum_1^m \theta_j = 1$$

and $\mathbf{s}_*$ is a point on the intersection of a $k-m$ dimensional face of the polyhedron with the ball $|\mathbf{s}_*| = R_{i_0}$ (see Figure B.2.) Geometrically this says that $\mathbf{u}_*$ is a stationary point if one forward Euler step *backward* in time from $\mathbf{s}_*$ can reach the simplex which is dual to the intersection set (the convex combination of the centers $\mathbf{u}_{i_j}$) of the balls which intersect. This is the same as Guckenheimer and Vladimirsky's [12] upwinding condition.

Not all stationary points are minimizers, and we must next determine the stability of the sytationary point (the second order optimality conditions). The stationary point lies on the set of points determined by the active constraints (the m spheres on which it lies). If $m \leq k$ this set is a sphere of dimension $k-m$ in a hyperplane orthogonal to the dual simplex of the intersection, whose center is a point interior to the dual simplex. The second order necessary conditions for a minimum [4] are that for any vector $\mathbf{s}$ in the tangent space of the intersection of the m constraints, the product

$$\mathbf{s}^T \Phi_{i_0}^T \mathbf{F}_\mathbf{u} \Phi_{i_0} \mathbf{s} - 2 \sum_0^{j<m} \theta \mathbf{s}^T \mathbf{s} > 0.$$

or

$$\alpha \frac{\mathbf{s}^T \Phi_{i_0}^T \mathbf{F}_\mathbf{u} \Phi_{i_0} \mathbf{s}}{R_{i_0}^2} > 1.$$

Now α is the distance, relative to the length of the flow vector, from the extrema to the dual simplex. So $\alpha|\mathbf{F}|$ is a fraction of the radius of the ball. The radius of each ball is chosen so that $\mathbf{F}$ varies on the order of ϵ on the scale of the balls, so the stationary point is a saddle unless $m = k$ (when there are no $\mathbf{s}$ vectors and the sphere is a pair of points). In other words, a stationary point lies on a sphere whose center is further *back* in time, so points on the sphere are "better" than the stationary point, unless the sphere is a single point (i.e. $m = k$).

Appendix C. An expansion for the stable and unstable Manifolds of a hyperbolic Fixed Point .

In this section we derive expansions for the invariant manifolds associated with a hyperbolic fixed point of the flow from this local representation. This has been done before by Beyn and Kleß[3], Simó [29], and Eirola and Pfaler [8]. We summarize it here because our notation is significantly different.

In the previous section we used an explicit initial global parameterization for the invariant manifold, but an equivalent local condition can be given by observing that at each point on the manifold the vector F must lie in the tangent plane of the manifold. If the invariant manifold is described by $u(s)$, with the fixed point at $\mathbf{s} = 0$, and is dimension k, $\mathbf{u}' = \mathbf{F}$ becomes

$$F^i(u(s)) = u^i_{,j}(s) a^j(s) \tag{C.1}$$

with $a^j = \partial s^j/\partial t$. This form has been used to compute invariant Tori (see Moore [27], and Dieci and Lorenz [6]).

We will assume that:

1. u^i is a fixed point, so that at u^i, $F^i = 0$.
2. $u^i_{,j}$ is a basis for an invariant subspace of the Jacobian $F^i_{,j}$ at the fixed point. That is, there are cofficients $a^i_{,j}$ such that
$$F^i_{,p}u^p_{,j} = a^p_{,j}u^i_{,p} \qquad \longrightarrow \qquad a^i_{,j} = g^{iw}u^p_{,w}F^p_{,q}u^q_{,j}$$
(recall that g^{ij} is the inverse of the metric $u^p_{,i}u^p_{,j}$.)
3. v^i_j is a basis for the orthogonal complement of the invariant subspace, so that
$$v^p_i F^p_{,q} u^q_{,j} = 0$$

Then Eq. (C.1) and its derivatives are

$$F^i = u^i_{,p}a^p$$

$$F^i_{,p}u^p_{,j} = u^i_{,p,j}a^p + u^i_{,p}a^p_{,j}$$

$$F^i_{,p,q}u^p_{,j}u^q_{,k} + F^i_{,p}u^p_{,j,k} = u^i_{,p,j,k}a^p + u^i_{,p,j}a^p_{,k} + u^i_{,p,k}a^p_{,j} + u^i_{,p}a^p_{,j,k}$$

$$F^i_{,p,q,r}u^p_{,j}u^q_{,k}u^r_{,l} + F^i_{,p,q}(u^p_{,j,l}u^q_{,k} + u^p_{,j,k}u^q_{,l} + u^p_{,j}u^q_{,k,l}) + F^i_{,p}u^p_{,j,k,l} =$$
$$u^i_{,p,j,k,l}a^p + u^i_{,p,j,k}a^p_{,l} + u^i_{,p,k,l}a^p_{,j} + u^i_{,p,j,l}a^p_{,k}$$
$$+u^i_{,p,j}a^p_{,k,l} + u^i_{,p,l}a^p_{,j,k} + u^i_{,p,k}a^p_{,j,l} + u^i_{,p}a^p_{,j,k,l}$$

At the fixed point we choose $a^p = 0$, and along with the assumptions, this satisfies the first two equations. The basis for the invariant subspace and the basis for the orthogonal complement together are a basis for the entire space, so the remaining equations are zero if and only if the projection of each onto the basis vectors is zero.

We choose a parameterization which is Euclidean in the tangent space, that is $g_{ij} = \delta_{ij}$ and $\Gamma_{ijk} = 0$. We then have that

$$\Gamma_{ijkl} = (\Gamma_{ijk})_{,l} - \Gamma_{pil}\Gamma^p_{jk} - \eta_{pil}\eta^p_{jk} = -\eta_{pil}\eta^p_{jk}$$

and to third order

$$u^i(s) \sim u^i + \left(s^j - \frac{1}{6}\eta^p_{jw}\eta_{pqr}s^q s^r s^w\right)u^i_{,j} + \left(\frac{1}{2}\eta^j_{pq}s^p s^q + \frac{1}{6}\eta^j_{pqr}s^p s^q s^r\right)v^i_j$$

Here (recall that double indices indicate a summation) –

η_{ijk} is the solution of the $(n-m)m^2$ dimensional linear system–

$$u^r_{,w}F^r_{,q}u^q_{,k}\eta_{iwj} + u^r_{,w}F^r_{,q}u^q_{,j}\eta_{iwk} - v^r_i F^r_{,p}v^p_q\eta^q_{jk} = v^r_i F^r_{,p,q}u^p_{,j}u^q_{,k}.$$

Let

$$a^i_{,j,k} = u^w_{,i}F^w_{,p,q}u^p_{,j}u^q_{,k} + u^p_{,i}F^p_{,q}v^q_r\eta_{rjk}$$

Then $\eta^i_{,j,k,l}$ is the solution of the $(n-m)m^3$ dimensional linear system–

$$u^q_{,p}F^q_{,r}u^r_{,l}\eta_{ipjk} + u^q_{,p}F^q_{,r}u^r_{,j}\eta_{ipkl} + u^q_{,p}F^q_{,r}u^r_{,k}\eta_{ipjl} - v^q_i F^q_{,r}v^r_w\eta^w_{jkl} =$$
$$v^w_i F^w_{,p,q,r}u^p_{,j}u^q_{,k}u^r_{,l} + v^w_i F^w_{,p,q}v^p_r u^q_{,k}\eta_{rjl}$$
$$+v^w_i F^w_{,p,q}v^p_r u^q_{,l}\eta_{rjk} + v^w_i F^w_{,p,q}u^p_{,j}v^q_r\eta_{rkl}$$
$$-\eta_{ipj}a^p_{,k,l} - \eta_{ipl}a^p_{,j,k} - \eta_{ipk}a^p_{,j,l}$$

Acknowledgements

The author would like to thank H. Osinga, B. Krauskopf and A. Vladmirisky for many useful and enjoyable discussions of the issues involved in computing invariant manifolds, and A. Conn and A. Waechter for discussions about constrained nonlinear optimization on the boundary of a union of spherical balls.

Much of the originally motivation for this work was the author's desire to replicate the extraordinary drawings in the series of books by Abraham and Shaw [1].

The figures here were made using DataExplorer (`opendx.org`), and AutoSketch®.

REFERENCES

[1] Ralph E Abraham and Christopher D Shaw. *Dynamics – The Geometry of Behavior*. Ariel Press, Inc., Santa Cruz, 1982.

[2] J. J. Allen and B. Auvity. Interaction of a vortex ring with a piston vortex. *Journal of Fluid Mechanics*, 465:353–378, August 2002.

[3] Wolf-Jürgen Beyn and Winfried Kleß. Numerical Taylor expansions of invariant manifolds in large dynamical systems. *Numerische Mathematik*, 80(1):1–38, 1998.

[4] Andrew R. Conn, Nicholas I. M. Gould, and Philippe L. Toint. *Trust Region Methods*. MPS-SIAM series on Optimization. SIAM and MPS, Philadelphia, 2000.

[5] Michael Dellnitz and Andreas Hohmann. A subdivision algorithm for the computation of unstable manifolds and global attractors. *Numerische Mathematik*, 75:293–317, 1997.

[6] Luca Dieci and Jens Lorenz. Computation of invariant tori by the method of characteristics. *SIAM J. Numer. Anal.*, 32(5):1436–1474, October 1995.

[7] Eusebius J. Doedel. Private Communication.

[8] Timo Eirloa and Jan von Pfaler. Numerical expansioons for invariant manifolds. Technical Report A460, Helsinki University of Technology Institute of Mathematics, 2003.

[9] Luther Pfahler Eisenhart. *Riemannian Geometry*. Princeton University Press, Princeton, New Jersey, 1925.

[10] G. Gomez, W. S. Koon, M. W. Loi, J. E. Marsden, J. Masdemont, and S. D. Ross. Invariant manifolds, the spatial three-body problem and space mission design. In *International Conference on Differential Equations*, pages 1167–1181, Berlin, 1999.

[11] John Guckenheimer. A strange, strange attractor. In J. E. Marsden and M. McCracken, editors, *The Hopf Bifurcation and its Applications*, number 19 in Applied Mathematical Sciences, pages 368–381. Springer, 1976.

[12] John Guckenheimer and Alexander Vladimirsky. A fast method for approximating invariant manifolds. submitted to SIAM J. Appl. Dyn. Systems, 2003.

[13] John Guckenheimer and Patrick Worfolk. Dynamical systems: Some computational problems. In D. Schlomiuk, editor, *Bifurcations and Periodic Orbits of Vector Fields*, pages 241–277. Kluwer Academic Publishers, 1993.

[14] Jack K. Hale. *Ordinary Differential Equations*. Pure and Applied Mathematics. Wiley Interscience, New York, 1969.

[15] Michael E. Henderson. Multiple parameter continuation: Computing implicitly defined k–manifolds. *International Journal of Bifurcation and Chaos*, 12(3):451–476, 2002.

[16] K. C. Howell, B. T. Barden, and M. W. Lo. Application of dynamical systems theory to trajectory design for a libration point mission. *The Journal of the Astronautical Sciences*, 45(2):161–178, April–June 1997.

[17] J. P. M. Hultquist. Constructing stream surfaces in steady 3D vector fields. In *IEEE Proceedings Visualization '92*, pages 171–178, Boston, October 1992.

[18] E Atlee Jackson. *Perspectives of Nonlinear Dynamics, Volume 1*. Cambridge University Press, Cambridge, 1990.

[19] E Atlee Jackson. *Perspectives of Nonlinear Dynamics, Volume 2*. Cambridge University Press, Cambridge, 1990.

[20] Mark E. Johnson, Michael S. Jolly, and Ioannis G. Kevrekidis. Two-dimensional invariant manifolds and global bifurcations: some approximation and visualization studies. *Numerical Algorithms*, 14:125–140, 1997.

[21] B. Krauskopf and H. Osinga. Globalizing two-dimensional unstable manifolds of maps. *International Journal of Bifurcation and Chaos*, 8(3):483–503, 1998.

[22] Bernd Krauskopf and Hinke M. Osinga. Two-dimensional global manifolds of vector fields. *Chaos*, 9(3):768–774, 1999.

[23] Bernd Krauskopf and Hinke M. Osinga. Visualizing the structure of chaos in the lorenz system. *Computers & Graphics*, 26(5):815–823, 2002.

[24] Bernd Krauskopf and Hinke M. Osinga. The lorenz manifold as a collection of geodesic level sets. *Nonlinearity*, 17:C1–C6, 2004.

[25] T. Leweke and C. H. K. Williamson. The long and short of vortex pair instability. *Physics of Fluids*, 8(9):55–58, September 1998.

[26] David Lovelock and Hanno Rund. *Tensors, Differential Forms, and Variantional Principles*. John Wiley & Sons, New York, 1975.

[27] Gerald Moore. Computation and parameterization of invariant curves and tori. *SIAM J. Numer. Anal.*, 33(6):2333–2358, December 1996.

[28] Gerik Scheuermann, Tom Bobach, Hans Hagen, Karim Mahrous, Bernd Hamann, Kenneth I. Joy, and Wolfgang Kollmann. A tetrahedra-based stream surface algorithm. In *IEEE Proceedings Visualization '01*, pages 151–158, San Diego, October 2001.

[29] Carles Simó. On the numerical and analytical approximation of invariant manifolds. In D. Benest and C. Froeschlé, editors, *Les Methodes Modernes de las Machanique Céleste*, pages 285–329. Goutelas Academic Publishers, 1989.

[30] Colin Sparrow. *The Lorenz Equations: Bifuractions, Chaos and Strange Attractors*. Number 41 in Applied Mathematical Sciences. Springer, New York, 1982.

[31] Michael Spivak. *A Comprehensive Introduction to Differential Geometry, Volume 2*. Publish or Perish, Berkeley, 1970.

[32] Martin Stämpfle. Dynamical systems flow computation by adaptive triangulation methods. *Computing and Visualization in Science*, 2:15–24, 1999.

[33] Jarke J. van Wijk. Flow visualization with surface particles. *IEEE Computer Graphics and Applications*, 13(4):18–24, July 1993.

[34] Jarke J. van Wijk. Implicit stream surfaces. In *IEEE Proceedings Visualization '93*, pages 245–252, San Jose, October 1993.

[35] Thomas M. Whittaker. Automated streamline analysis. *Monthly Weather Review*, 105(6):786–788, June 1977.

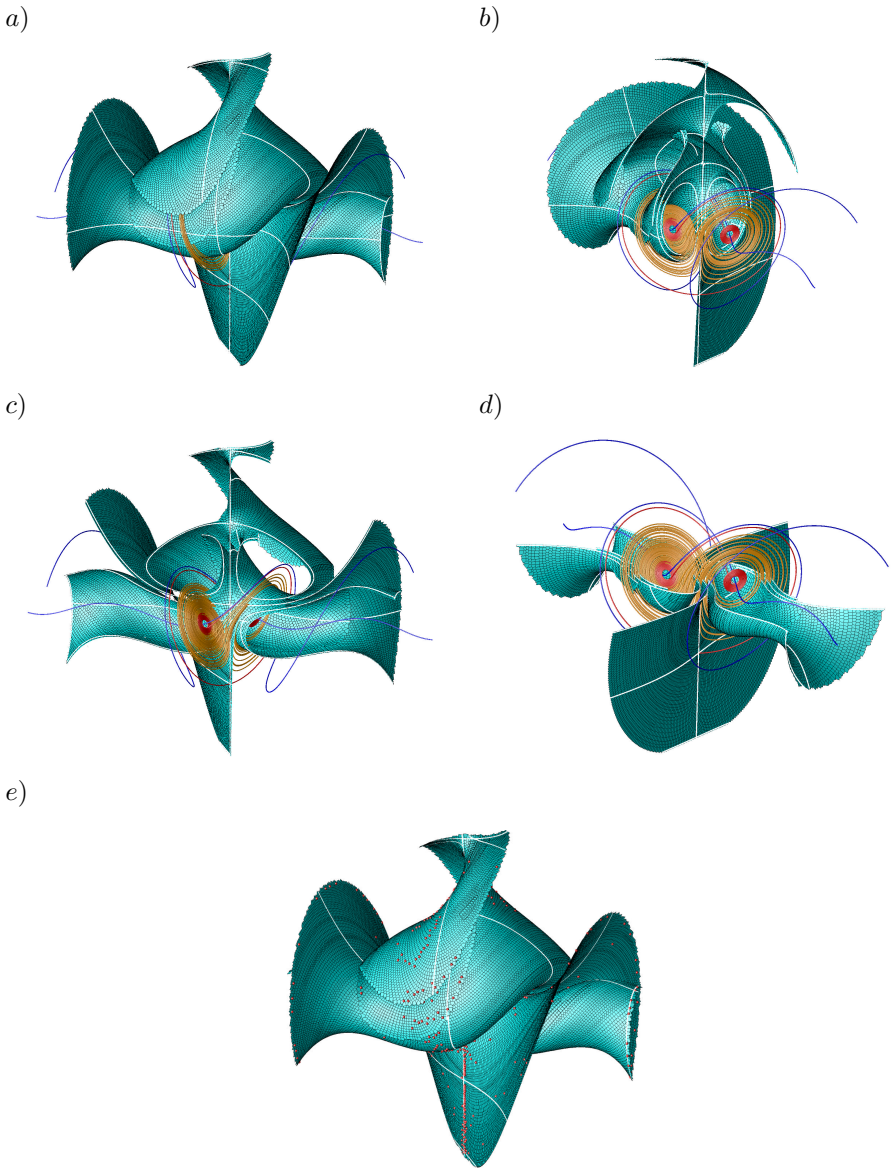

FIG. 5.2. *The stable manifold of the origin in the Lorenz system at the standard parameters* $\sigma = 10$, $\rho = 28$ *and* $\beta = 8/3$. *The scaled time* τ *was limited at 150, the total number of balls was 40,025 with 801 interpolation points. With 24 trajectories starting on* $\mathbf{c}(\sigma)$ *this means that the surface is covered with 825 fat trajectories. Also shown are the polygons used to tile the surface, and several lines on the surface. This run took about 13 minutes elapsed time on an IBM RS/6000 with a POWER3 processor and 256MB of memory.*

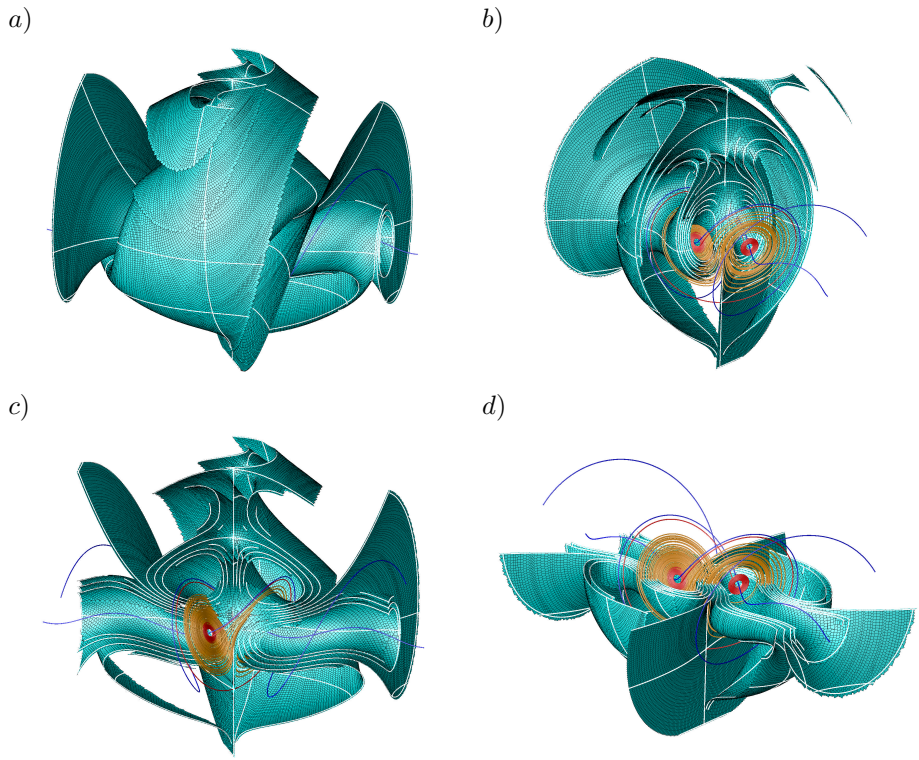

FIG. 5.3. *The stable manifold of the origin in the Lorenz system with $\sigma = 10$, $\rho = 28$ and $\beta = 8/3$. The time τ was limited at 240, the total number of balls was 124,120 with 2238 interpolation points. With 24 trajectories starting on $\mathbf{c}(\sigma)$ this means that the surface is covered with 2,262 fat trajectories. Also shown are the polygons used to tile the surface, and several lines on the surface. This run took about 2.3 hours elapsed time.*

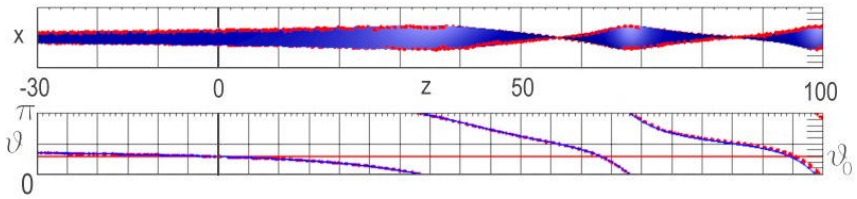

FIG. 5.4. *A comparison of the $u^i_{,1}$ tangent along the z-axis computed directly along the z-axis (see Figure 5.1) (blue), and measured from the results of the computation of the entire manifold (red). The z-axis is not contained in the entire manifold, instead is sampled on interpolated trajectories. The agreement is very good, though some deviation is noticable as z nears 100.*

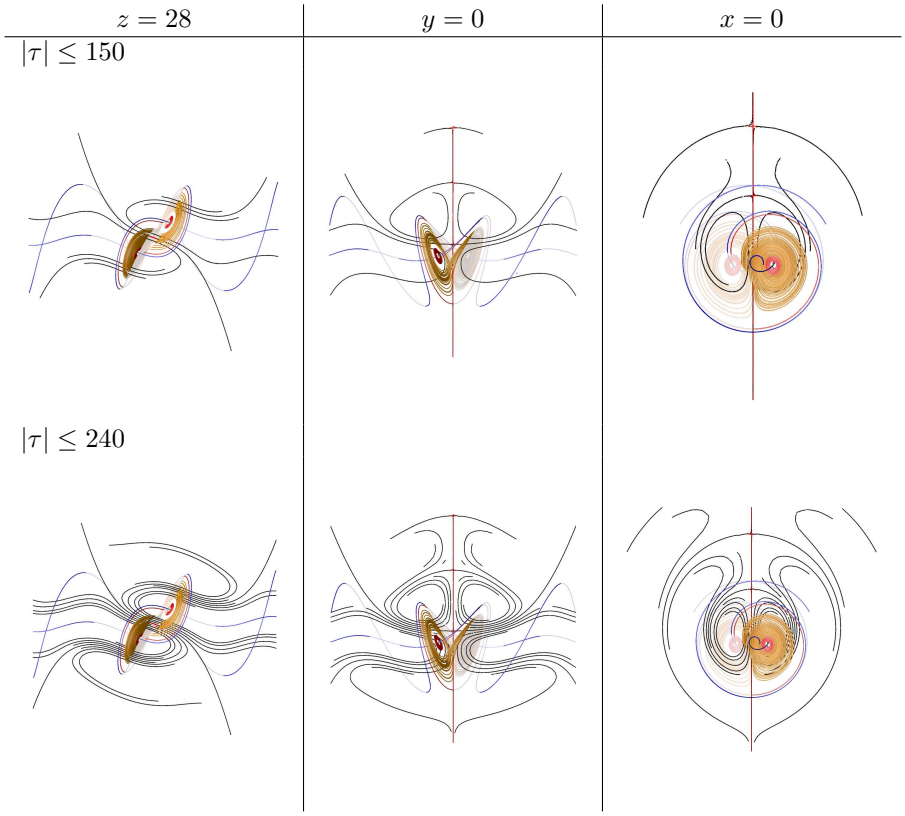

FIG. 5.5. *Sections of the stable manifold of the origin in the Lorenz system. The orange trajectory is near the attractor, and the blue and red lines are the stable manifold of the fixed points at $z = 28$ and unstable manifolds of the origin respectively.*

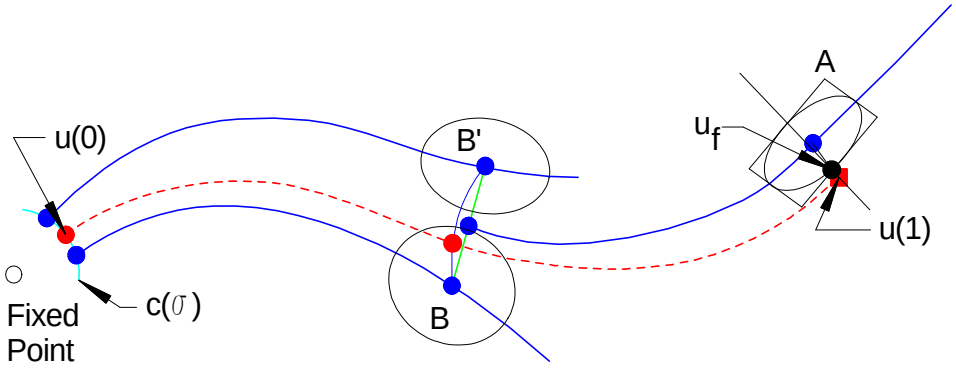

FIG. 6.1. *An sketch of how the accuracy of the algorithm might be measured. A point $\mathbf{u}_f$ on the approximate manifold is chosen, which lies on a chart whose center lies on a trajectory beginning on $\mathbf{c}(\sigma)$ or interpolated from the centers of k charts. The red trajectory starts on $\mathbf{c}(\sigma)$ and ends at a point whose projection onto chart A is $\mathbf{u}_f$. A nonsingular two point boundary value problem can be written for the red trajectory.*

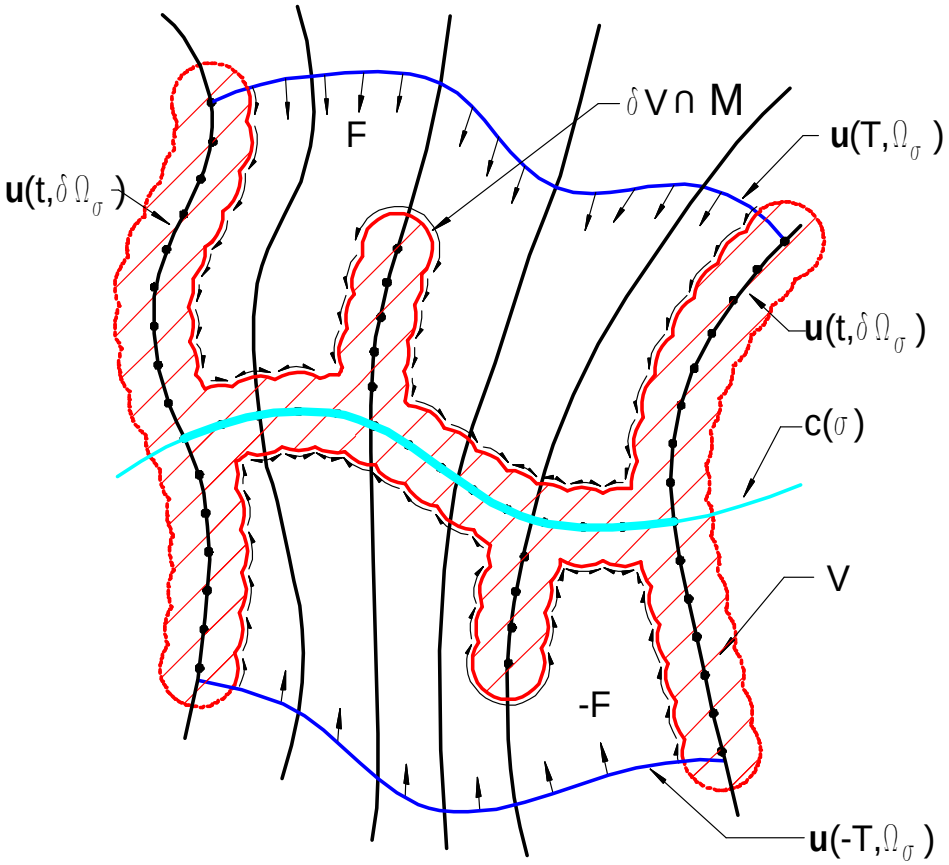

FIG. B.1. *A 2d example of the feasible region of the optimization problem posed in Appendix B. A section of the manifold of starting points (cyan) has been covered, as has the image of the boundary of that section under the flow. On the image of the section up to some time T this defines a region in which trajectories are contained. In the interior "descent" is backward along trajectories, and on the boundary we use the backward flow to induce a flow on the boundary.*

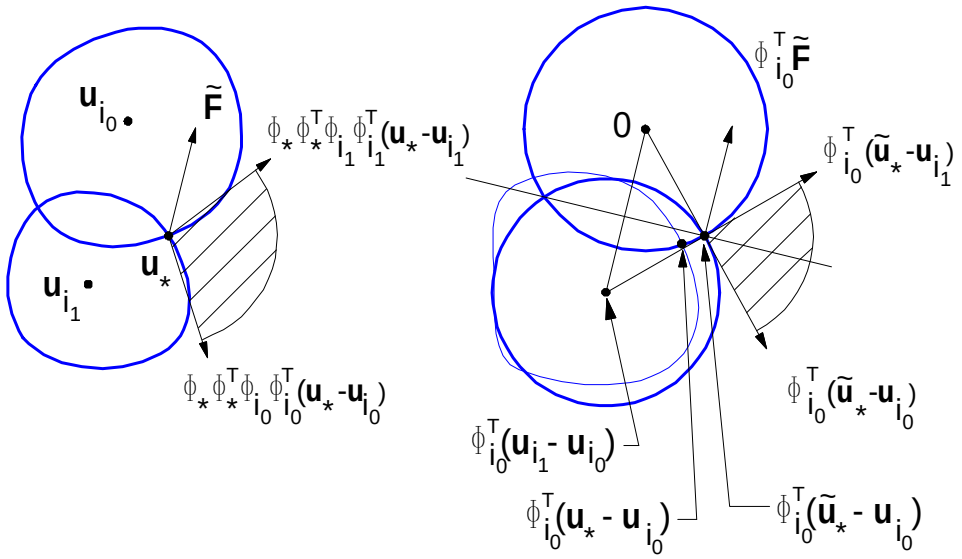

FIG. B.2. *The stationarity conditions require that a point be a stable fixed point under the induced flow on the boundary. A point is a fixed point if the flow lies in the positive cone of normals to the boundary (left). We approximate this by projecting into the tangent space of one of the boundary balls (right) and replace projected balls by balls of the same radius at the projected centers.*

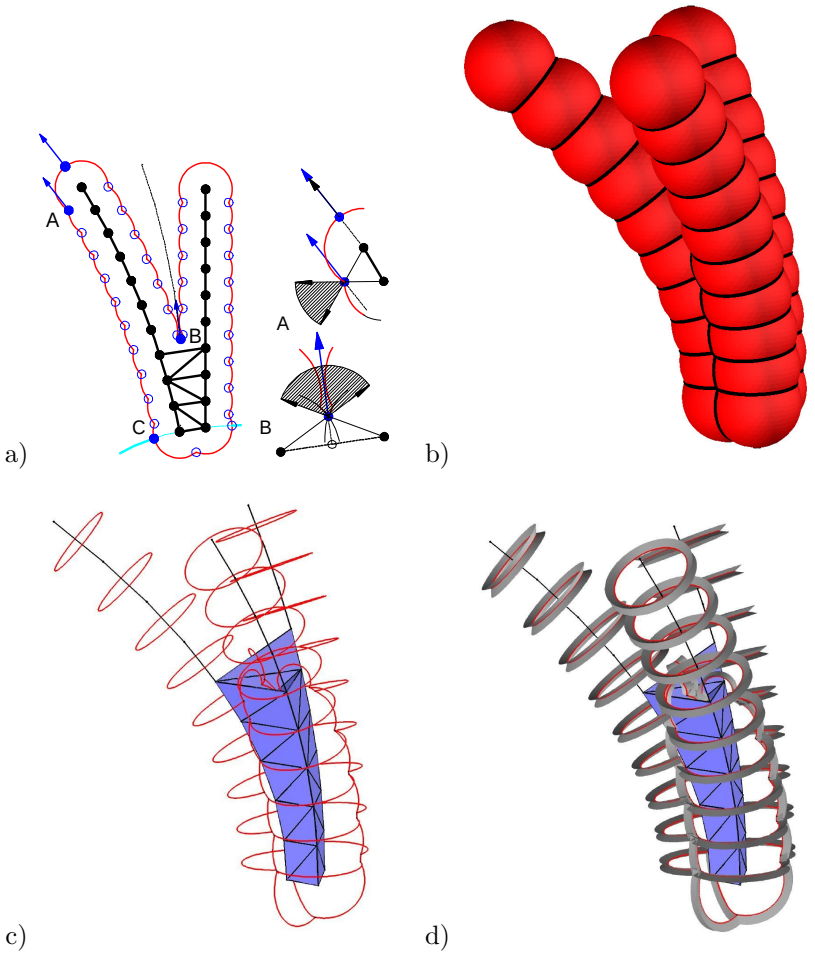

FIG. B.3. *Finding stationary points on the surface of a union of spherical balls. a) The 2d case. A shows two stationary points, neither of which is stable. The one on the circle of intersection is not in the shaded cone, the one on the top is near where the trajectory leaves the balls, and lies on a circle whose center is backward in time (so other points on the circle are closer to* **c**). *B shows a stable fixed point. Values for starting a fat trajectory passing near B can be interpolated from the dual simplex. b) The balls in a 3d example. c) The intersections of the balls and the dual complex. d) The "cones" for stationarity. The flow must lie in a fan, which is the cross section of the v-shaped groves and the plane containing the axis of the circle and the point on the circle.*